

Development of Universal Biosensing Platforms Based
on CRISPR/Cas12a systems

Yongya Li, BSc

Chemistry (Inorganic)

Submitted in partial fulfillment of the requirement for the degree of
Master of Science

Faculty of Mathematics & Science, Brock University

St. Catharines, Ontario

© 2020

Abstract

CRISPR/Cas technologies possess the promising potential to affect biosensing field by providing a sensitive, precise, rapid, versatile and cost-effective method for diverse target detections. This thesis focusses on the development of CRISPR/Cas12a based biosensing platforms for nucleic acid and protein detection. Two distinct CRISPR/Cas based diagnostic methods were developed. The first developed method is a plasmonic CRISPR Cas12a assay for colorimetric detection of viral nucleic acid. This assay generates colorimetric signals for nucleic acid amplicons by combining the unique target-induced collateral cleavage activity of Cas12a with plasmon coupling of DNA functionalized gold nanoparticles. The practical applications of this assay were successfully demonstrated through the nucleic acid detection of hepatitis B virus (HBV) and Grapevine Red-Blotch Virus (GRBV). The second developed method is a universal proximity CRISPR Cas12a assay for ultrasensitive detection of nucleic acids and proteins. The target recognition is achieved through proximity binding rather than direct CRISPR/Cas 12a recognition, allows the flexible assay design and expansion to target diverse targets. This assay was successfully adapted to detect nucleic acids and antibodies in both buffer and diluted human serum.

Acknowledgement

I am grateful to Brock University and the Department of Chemistry for allowing me to pursue graduate studies. I would like to send the most profound gratitude to my supervisor, Prof. Feng Li, and committee members, Prof. Melanie Pilkington and Prof. Travis Dudding, for exemplary guidance and constant encouragement throughout my thesis project. I also thank all the groupmates in Prof. Li group for training and guiding me during my research project period. I would like to thank Prof. Adam Macneil, Colton Watson, Tony Wang and Sudarsana Poojari for providing samples to validate my assays.

Table of Contents

Abstract	I
Acknowledgements	II
Table of Contents	III
List of Figures	VI
List of Tables	VIII
List of Schemes	VIII
List of Abbreviations	IX
Chapter 1 CRISPR/Cas Systems for Biosensing Applications	1
1.1 Introduction	1
1.2 Classification of CRISPR/Cas Biosensing Systems	2
1.3 CRISPR/Cas-based Biosensing Systems	5
1.3.1 (d)Cas9 Effector-based CRISPR/Cas Biosensing Systems	5
1.3.2 Cas12 Effector-based CRISPR/Cas Biosensing Systems	14
1.3.3 Cas14 Effector-based CRISPR/Cas Biosensing Systems.....	18
1.3.4 Cas13 Effector-based CRISPR/Cas Biosensing Systems.....	19
1.4 Present Challenges and Conclusions	22
Chapter 2 A Universal Plasmonic CRISPR Cas12a Assay for Field-Deployable Viral Diagnostics	26
Contribution Statement	26
2.1 Introduction	26
2.2 Materials and Methods	28
2.2.1 Materials	28
2.2.2 DNA Sequence and Modifications	29
2.2.3 Experimental Procedures	31
2.2.3.1 Preparation of DNA Functionalized AuNPs	31
2.2.3.2 Plasmonic Assay Protocol	31
2.2.3.3 Plasmonic CRISPR-Cas12a Assay	32
2.2.3.4 PCR Protocol	32
2.2.3.5 Polyacrylamide Gel Electrophoresis (PAGE).....	32
2.2.3.6 Grapevine Sample Collection and DNA Extraction	32

2.2.3.7 Grapevine Sample Testing Using Droplet Digital PCR (ddPCR) and End-Point PCR	33
2.3 Result and Discussion	34
2.3.1 Assay Principle	34
2.3.2 Condition Optimizations	36
2.3.3 Assay Validation for GRBV Infections Diagnostics	38
2.3.4 Assay Validation for HBV Plasmids Detection	44
2.4 Conclusion	46
Chapter 3 A Universal Proximity CRISPR Cas12a Assay for Ultrasensitive Detection of Nucleic Acids and Proteins	47
Contribution Statement	47
3.1 Introduction	47
3.2 Materials and Methods	49
3.2.1 Materials	49
3.2.2 DNA Sequence and Modifications	49
3.2.3 Experimental Procedures	50
3.2.3.1 Nucleic Acid Detection Using Proximity CRISPR Cas12a Assay	50
3.2.3.2 Proximity CRISPR Cas12a Assay with Blocking DNA	50
3.2.3.3 Antibody Detection Using Proximity CRISPR Cas12a Assay	51
3.3 Result and Discussion	51
3.3.1 Assay Principle Illustration	51
3.3.2 Nucleic Acids Detections	53
3.3.3 Proteins Detections	58
3.4 Conclusion	62
Chapter 4 Conclusion and Future Work	64
References	65

List of Figures:

Figure 1.1 CRISPR/Cas9 systems to detect and cleavage double-stranded DNA.	3
Figure 1.2 NASBA-CRISPR Cleavage (NASBACC) applied to distinguish between American and African viral RNA strains with a single-base difference.	6
Figure 1.3 CRISPR-typing PCR (ctPCR) used to detect and type HPV DNA.	7
Figure 1.4 Overview of the Finding Low Abundance Sequences by Hybridization (FLASH).	8
Figure 1.5 Cas9 triggered isothermal exponential amplification reaction (CAS-EXARP).	9
Figure 1.6 Schematic reaction process of CRISPR–Cas9-triggered strand displacement amplification method (CRISDA) method.	11
Figure 1.7 RNA-guided featured DNA detection by the paired dCas9 (PC) reporter method.	12
Figure 1.8 Overview of the Rolling Circle Amplification (RCA)-CRISPR-split-Horseradish peroxidase (HRP) (RCH) method.	13
Figure 1.9 CRISPR–Chip for unamplified gene detection.	14
Figure 1.10 DNA endonuclease targeted CRISPR trans reporter (DETECTR) system.	15
Figure 1.11 Schematic illustration of one-Hour Low-cost Multipurpose highly Efficient System (HOLMES) for DNA detection and SNP genotyping.	16
Figure 1.12 Schematic workflow and applications of one-Hour Low-cost Multipurpose highly Efficient System version 2 (HOLMESv2).	17
Figure 1.13 Schematic of E-CRISPR for nucleic acid detection.	18
Figure 1.14 Diagram of Cas14-DETECTR strategy.	19
Figure 1.15 Schematic of Specific High-Sensitivity Enzymatic Reporter UnLOCKing (SHERLOCK).	20
Figure 1.16 Schematic of Specific High-Sensitivity Enzymatic Reporter UnLOCKing version 2 (SHERLOCKv2).	21
Figure 2.1 AuNP-based plasmonic readout.	36

Figure 2.2 Optimal condition for the plasmonic assay in the presence of CRISPR Cas12a.	37
Figure 2.3 Plasmonic CRISPR Cas12a assay.	38
Figure 2.4 Representative symptoms of grapevine red blotch virus infections on the leaves of red-fruited (Cabernet Franc, left) and white-fruited (Chardonnay, right) <i>Vitis Vinifera</i>	39
Figure 2.5 Visual detection of GRBV infection in grape samples using PCR and plasmonic CRISPR Cas12a assay.	40
Figure 2.6 Visual analysis of PCR amplicons using the plasmonic CRISPR Cas12a assay.	41
Figure 2.7 PAGE analysis of PCR amplicons of GRBV infected grape samples (V1, V2, V3) and health grape controls (H1, H2).	41
Figure 2.8 Detection of GRBV isolates by end-point PCR and electrophoresis.	42
Figure 2.9 Visual detection of GRBV infected grapevine leaf samples using PCR and plasmonic CRISPR Cas12a assay.	43
Figure 2.10 Visual detection of HBV DNA using LAMP and plasmonic CRISPR Cas12a assay.	45
Figure 3.1 Proximity CRISPR Cas12a assay for the detection of nucleic acids.	55
Figure 3.2 quantitative profiling of IL-6 expression during allergen-mediated mast cell activation using proximity CRISPR Cas12a assay.	56
Figure 3.3 Quantitative profiling of allergen-mediated mast cell activation in three independent cultures of BMMCs.	57
Figure 3.4 Estimated melting temperature (T_m) between P1' and P2' in the absence or presence of the target antibody.	58
Figure 3.5 Proximity CRISPR Cas12a assay for the detection of antibodies.	60
Figure 3.6 Optimization of the concentrations of proximity probes P1' and P2' for protein analysis.	61
Figure 3.7 Optimization of the concentrations of DNA polymerase (Klenow Fragment, unit) for protein analysis.	61

Figure 3.8 Optimization of nicking endonuclease for the proximity CRISPR Cas12a assay. 62

List of Tables:

Table 1.1 Summary of the nucleic acid targets and collateral activities of CRISPR-Cas proteins. 4

List of Schemes:

Scheme 2.1 Schematic illustration of the plasmonic CRISPR Cas12a assay for field-deployable nucleic acid testing. 35

Scheme 3.1 Schematic illustration of the proximity CRISPR Cas12a assay for the amplified detection of nucleic acids. 52

List of Abbreviations:

CRISPR	clustered regularly interspaced short palindromic repeats
Cas	CRISPR-associated
gRNA	guide RNA
PAM	protospacer-adjacent motif
dCas9	deactivated Cas9
crRNA	CRISPR RNA
tracrRNA	trans-activating crRNA
sgRNA	single-guide RNA
dsDNA	double-stranded DNA
SpCas9	<i>Streptococcus pyogenes</i> Cas9 protein
ssDNA	single-stranded DNA
ssRNA	single-stranded RNA
NASBA	nucleic acid sequence-based amplification
PCR	polymerase chain reaction
SDA	strand displacement amplification
EXPAR	exponential amplification reaction
FLASH	finding low abundance sequences by hybridization
NASBACC	nucleic acid sequence-based amplification CRISPR/Cas9 Cleavage
fM	femtomolar
HPV	human papilloma virus
ctPCR	CRISPR-typing PCR
gs-primers	general-specific primers
NGS	Next Generation Sequencing
PAMmers	PAM-presenting oligonucleotides
NEase	Nicking endonuclease
aM	attomolar
CAS-EXARP	Cas9 triggered isothermal exponential amplification reaction
LAMP	loop-mediated isothermal amplification
CRISDA	CRISPR-Cas9-triggered Strand Displacement Amplification
nCas9	Cas9 nickases
SDA	single-strand displacement amplification
PNA	peptide nucleic acid
PLA	Proximity Ligand Assay
PC	Paired CRISPR/dCas9
RCA	Rolling Circle Amplification
HRP	Horseradish peroxidase
RCH	Rolling Circle Amplification (RCA)-CRISPR-split-Horseradish peroxidase (HRP)
DETECTR	DNA endonuclease targeted CRISPR trans reporter
RPA	recombinase polymerase amplification
FQ	fluorophore quencher

HOLMES	one-Hour Low-cost Multipurpose highly Efficient System
PRV	pseudorabies virus
JEV	Japanese encephalitis virus
HOLMESv2	one-Hour Low-cost Multipurpose highly Efficient System Version 2
SNP	single nucleotide polymorphism
E-CRISPR	electrochemical CRISPR/Cas-based biosensor
pM	picomolar
HPV-16	human papilloma virus 16
PB-19	parvovirus B19
SHERLOCK	Specific High-Sensitivity Enzymatic Reporter UnLOCKing
RT-RPA	reverse transcription recombinase polymerase amplification
HUDSON	heating unextracted diagnostic samples to obliterate nucleases
SARS	severe acute respiratory syndrome
HBV	hepatitis B virus
GRBV	grapevine red-blotch virus
qPCR	quantitative polymerase chain reaction
ssDNase	single-stranded DNase
AuNPs	gold nanoparticles
NAT	nucleic acid testing
PAGE	polyacrylamide gel electrophoresis
POC	point-of-care
T _m	melting temperature
LOD	limit of detection
PCR	polymerase chain reactions
CRISPR Dx	CRISPR diagnostics

Chapter 1: CRISPR/Cas Systems for Biosensing Applications

1.1 Introduction

Nowadays, the continuously increasing incidence and breakout of infectious diseases, antimicrobial resistance, food contamination and environmental pollution, especially in developing countries and resource-limited regions, underline the urgent need to develop novel molecular diagnostic approaches for biosensing, especially ones that can be used for rapid and versatile point-of-care (POC) diagnostic applications^{1,2}. Molecular diagnostic applications mainly focus on validating and quantifying biomarkers, such as nucleic acids and proteins, that has been continuously developed in the past few decades. However, most of the existing approaches require well-designed and sophisticated systems which limit applicability and universality. Therefore, simplicity and versatility remain key challenges for biosensing applications.

The clustered regularly interspaced short palindromic repeats (CRISPR) and CRISPR-associated (Cas) proteins have led a revolution in biology since the CRISPR/Cas9 system was firstly applied for gene editing in 2013^{3,4}. After that, CRISPR-Cas systems have been adapted for genetic engineering at an extraordinary pace in various organisms, including plants, animals and even human⁵⁻⁹. CRISPR/Cas based approaches are characterized by tunable specificity for diverse nucleic acid targets by simply changing guide RNA (gRNA) sequence, but do not require sophisticated systems or designs compared with those of conventional techniques, thus regarded as revolutionary gene-editing toolboxes.

To date, the revolution of CRISPR-Cas systems expands applications further into biosensing applications¹⁰. CRISPR-Cas systems were firstly utilized to detect nucleic acid for biosensing in 2016¹¹. Since then, CRISPR-Cas technology has opened the door to develop novel biosensing tools that offer cost-effective, versatile and portable diagnostics for diverse molecular targets. This review provides an overview of the classification of current CRISPR/Cas biosensing system with their properties, principles and applications, as well as the perspectives of CRISPR/Cas systems leading to the next generation biosensing techniques.

1.2 Classification of CRISPR/Cas Biosensing Systems

CRISPR/Cas systems naturally exist as adaptive immune systems in bacteria to against viral infection. The function of the CRISPR/Cas system relies on two key components: a CRISPR-associated protein (Cas protein) and a guide RNA (gRNA). The gRNA serves as the guider for a Cas protein to provide specific binding with the genomic target through RNA-DNA hybridization. The Cas protein, which processes target-dependent endonuclease activity, binds and cleaves nucleic acid target under the guidance of gRNA. The currently established CRISPR/Cas-based nucleic acid biosensing systems can be divided into 4 distinct classes based on Cas proteins (Cas9, Cas13, Cas12 and Cas14) with different characteristics¹²⁻¹⁴. Although their principles and performance are different, there are three key parts to establish a typical CRISPR/Cas biosensing system (signal amplification, signal-transducing and signal reporting)¹⁵.

The earliest established CRISPR/Cas-based biosensing systems utilized Cas9 or deactivated Cas9 (dCas9) to detect double-stranded DNA^{15,16}. The key difference of dCas9 compared with Cas9 is that two cleavage sites of dCas9 are deactivated; therefore, dCas9 only provides the binding to nucleic acid target without generating cleavage¹⁷. Cas9 protein targets double-stranded DNA by the means of CRISPR RNA (crRNA) and trans-activating crRNA (tracrRNA). Jinek et al. reduced the complexity of Cas9 systems by creating a single-guide RNA (sgRNA) component which combines crRNA and tracrRNA¹³. Cas9 protein detects double-stranded DNA (dsDNA) target site guided by sgRNA and generates blunt-ended double-stranded target DNA breaks. The most frequently used Cas9 protein is derived from *Streptococcus pyogenes* (SpCas9); however, SpCas9 can tolerate few base pair mismatches between sgRNA and target DNA so that it can cleave non-target DNA sequence similar to the target site and induce frequent off-target effect¹⁸.

Cas9 programmed by crRNA:tracrRNA duplex

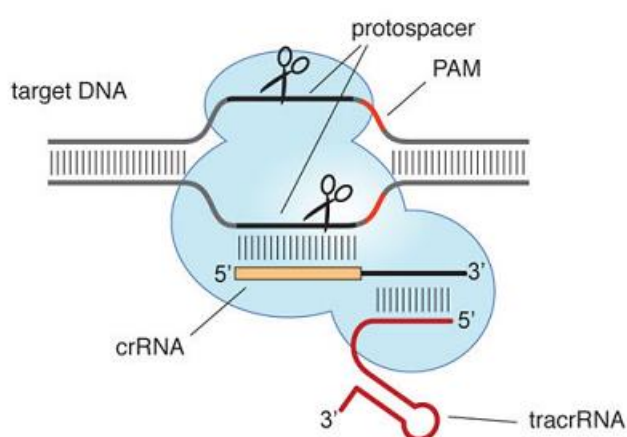


Figure 1.1 CRISPR/Cas9 systems to detect and cleavage double-stranded DNA (Reprinted with permission from Ref¹³, Copyright 2012, American Association for the Advancement of Science).

The late discovery of Cas proteins (Cas12¹⁹, Cas13²⁰ and Cas14²¹) with target-dependent collateral activity²¹⁻²³, which can be utilized as signal amplification or transducing, further improves the development of CRISPR/Cas-based biosensing systems. Compared with Cas9, Cas12a shows lower tolerance to the nucleotide mismatches between gRNA and target DNA so that it can provide higher accuracy²⁴. Moreover, Cas12a can detect both single-stranded DNA (ssDNA) and double-stranded DNA²³. Recently discovered Cas14 protein can detect single-stranded DNA in a PAM-sequence-independent manner which provides wider detectable sequence range²¹. Some Cas12 and Cas14 proteins possess target-dependent collateral activity: after binding target DNA, the proteins smash any adjacent DNA non-specifically^{21,23}. Cas13 proteins recognize single-stranded RNA (ssRNA), induce blunt-ended breaks, and indiscriminately degrade any adjacent ssRNA^{20,22}.

Cas Protein	Target	Collateral Activity
Cas9 (SpCas9)	dsDNA ¹³	
Cas12 (AsCas12a, AacCas12b)	dsDNA, ssDNA ¹⁹	ssDNA ²³
Cas14	dsDNA, ssDNA ²¹	ssDNA ²¹
Cas13 (LwaCas13a, PsmCas13b)	ssRNA ²⁰	ssRNA ²⁰

Table 1.1 Summary of the nucleic acid targets and collateral activities of CRISPR-Cas proteins.

1.3 CRISPR/Cas-based Biosensing Systems

1.3.1 (d) Cas9 Effector-based CRISPR/Cas Biosensing Systems

Cas9-based biosensing systems can be divided into two main categories, utilizing the target-specific cleavage behavior of Cas9 proteins or binding activity of dCas9 proteins. CRISPR/Cas9 based biosensing approaches are mainly relied on Cas9 site-specific cleavage integrating with emerging nucleic acid amplification strategies, such as nucleic acid sequence-based amplification (NASBA), polymerase chain reaction (PCR), strand displacement amplification (SDA), exponential amplification reaction (EXPAR) and finding low abundance sequences by hybridization (FLASH)^{2, 15}.

In 2016, Pardee et al. firstly integrated the programmable cleavage of the CRISPR/Cas9 system with NASBA to detect Zika virus RNA genome¹¹. NASBA is an isothermal RNA amplification technique for field-based diagnostic applications which involves reverse transcription, RNA degradation, dsDNA synthesis and DNA transcription²⁵. After the isothermal amplification of NASBA, RNA targets were converted into dsDNA products. Then sgRNA were designed to detect dsDNA targets by Cas9 proteins and the PAM site sequence was specific for American Zika but not African Zika genome. For American Zika, the cleaved dsDNA failed to activate a toehold switch sensor because the trigger sequence was lost after Cas9 cleavage and T7 RNA transcription. But African Zika contained an SNV on PAM site complementary sequence; therefore, Cas9 failed to generate cleavage so that the transcript RNA strand with trigger sequence could activate toehold switch sensor to induce color change^{11,26}. By deploying toehold switch sensors²⁶ on free-dried and paper-based platform, this

CRISPR/Cas9 approach (named NASBACC) achieved femtomolar (fM) sensitivity to discriminate between American and African viral RNA strains with a single-base difference.

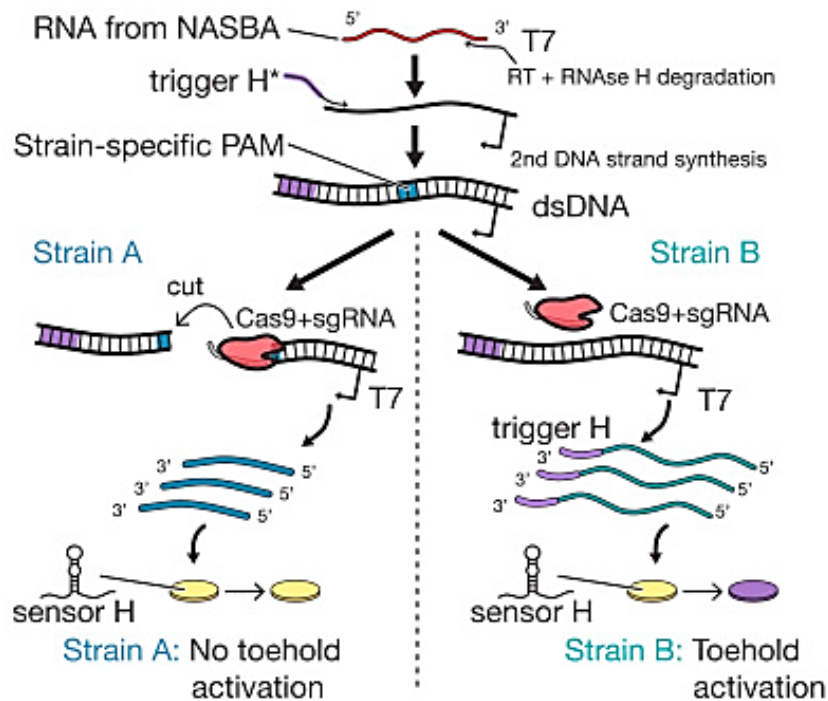


Figure 1.2 NASBA-CRISPR Cleavage (NASBACC) applied for distinguishing between American and African viral RNA strains with a single-base difference (Strain A: American Zika Virus Strain, Strain B: African Zika Virus Strain)¹¹ (Reprinted with permission from ref ¹¹, Copyright 2020, Elsevier).

In 2017, Wang et al. developed a method to detect and genotype human papillomavirus (HPV) DNA based on Cas9 protein and PCR, which was named CRISPR-typing PCR (ctPCR)²⁷. The detection process consists of three steps: (1) target DNA was amplified by using a pair of universal primers in the first round of PCR (PCR1); (2) the PCR1 products then were cleaved by sgRNA/Cas9 complexes, tailed by adenine (A), and ligated by T adaptors; (3) the treated PCR1 products were finally

amplified by using a pair of general-specific primers (gs-primers) in the second round of PCR (PCR2). PCR1 was designed to assay the target DNA (such as virus infection) and PCR2 was used to detect specific genotypes in target DNA (such as virus subtypes). This technique enabled distinguish HPV16 and HPV18 L1 gene from 13 different HPV subtypes.

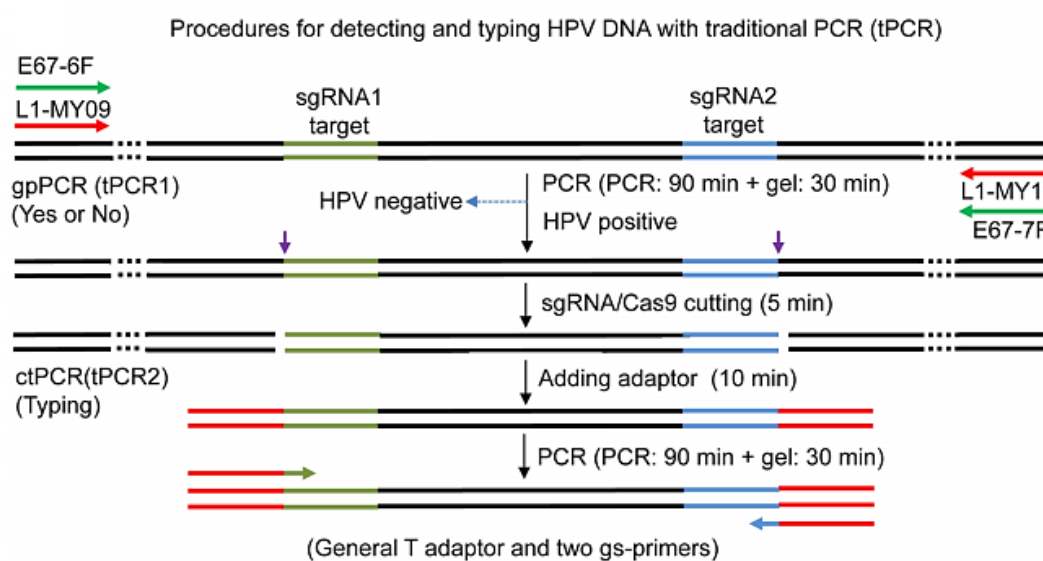


Figure 1.3 CRISPR-typing PCR (ctPCR) used to detect and type HPV DNA²⁷ (Reprinted with permission from ref ²⁷, Copyright 2018, Springer Nature).

Detection of antimicrobial resistance genes remains a challenge for nucleic acid detection due to its low abundance and unknown mutant sequence. To overcome this challenge, Quan et al. developed the Finding Low Abundance Sequences by Hybridization (FLASH) method to selectively amplify antimicrobial resistance genes with low abundance for Next Generation Sequencing (NGS)²⁸. FLASH utilized sgRNA/Cas9 complexes to cleave target of interest and followed by PCR amplification for NGS. Input DNA was firstly blocked by phosphate treatment to prevent ligation

with adapters, and then only target DNA was cut by sgRNA/Cas9 complexes to generate non-blocked ends that could be linked with universal adapters, amplified by PCR and sequenced by NGS. FLASH-NGS has been verified to detect the antimicrobial resistance genes in pneumonia-causing gram-positive bacteria and the drug resistance gene in the malaria parasite *Plasmodium falciparum*.

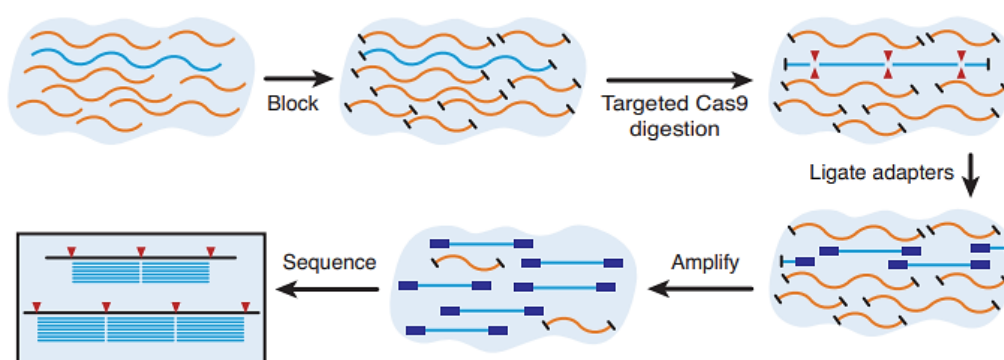


Figure 1.4 Overview of the Finding Low Abundance Sequences by Hybridization (FLASH)²⁸ (Reprinted with permission from ref ²⁸, Copyright 2019, Oxford University Press).

Isothermal amplification approaches are important for nucleic acid detection in POC or non-laboratory applications. Compared with conventional nucleic acid amplification reactions, Exponential Amplification Reaction (EXPAR) exhibits high amplification efficiency at isothermal condition, amplifying short single-stranded nucleic acids at 10^6 – 10^9 fold within minutes. However, the applications of EXPAR were limited because only short nucleic acid fragments can be applied as primers for amplification²⁹. In 2018, Huang et al. successfully utilized Cas9 cleavage activity to cut

nucleic acid targets into fragments for EXARP³⁰. Single-stranded DNA targets were cut into short fragments to generate primers by Cas9, utilizing a specifically designed PAM-presenting oligonucleotide (PAMmers). Primers then bind with templates, activated polymerase directed strand extension and produced the copies of primer sequence. Nicking endonuclease (NEase) induced single-strand nicking and released copied primers back to the amplification cycles. The amplified dsDNA products bind with SYBR Green I to generate real-time fluorescence signal. CAS-EXPAR has been applied to detect *Listeria monocytogenes* mRNA and DNA methylation with attomolar (aM) sensitivity and single-base specificity.

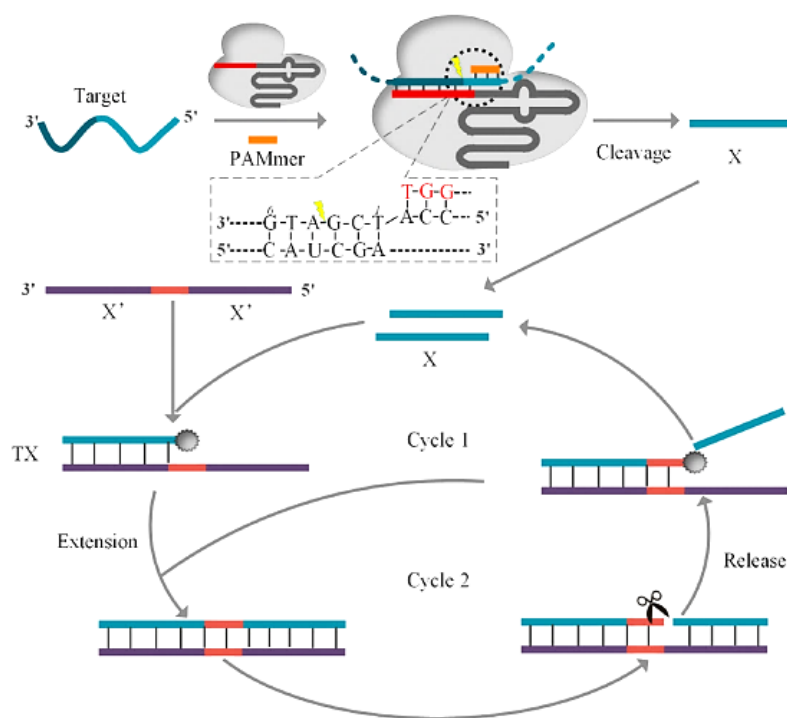


Figure 1.5 Cas9 triggered isothermal exponential amplification reaction (CAS-EXARP)³⁰ (Reprinted with permission from ref ³⁰. Copyright 2018, American Chemical Society).

Although many isothermal techniques have been proposed, such as nucleic acid sequence-based amplification (NASBA) and loop-mediated isothermal amplification (LAMP), these techniques still require an initial denaturation step to unwind the dsDNA structure of targets thereby limiting their practical applications. CRISPR-Cas9-triggered Strand Displacement Amplification (CRISDA) method utilized Cas9 nickases (nCas9 protein with a mutation of HNH catalytic residue that makes nCas9 lose endonuclease activity on DNA target strand) followed by isothermal single-strand displacement amplification (SDA) to unwind the dsDNA structure in target sequence range³¹. By integrating with peptide nucleic acid (PNA) invasion-endpoint measurement, CRISDA exhibited attomolar (aM) sensitivity and single-base specificity in the presence of a complex sample background.

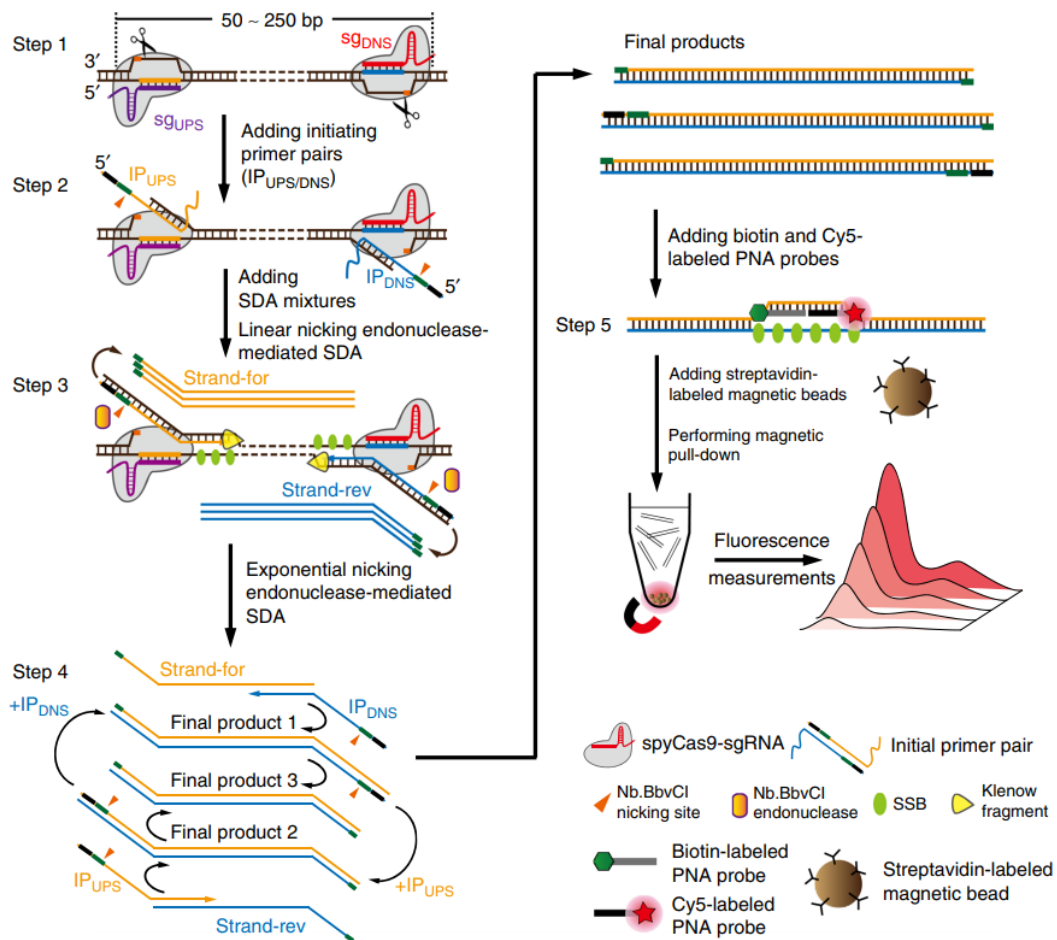


Figure 1.6 Schematic reaction process of CRISPR–Cas9-triggered strand displacement amplification method (CRISDA) method³¹ (Reprinted with permission from ref ³¹, Copyright 2018, Springer Nature).

On the other hands, CRISPR/dCas9 based biosensing systems utilize site-specific binding to provide the localization information of target sequence. One kind of dCas9 based assays follows a similar mechanism of Proximity Ligand Assay (PLA) utilizing two dCas9 proteins to target the sequence, which is in proximity, resulting in the dimerization of the ligation fused to dCas9 proteins and signal reporting. One example is that Chunbo Lou’s group developed the Paired CRISPR/dCas9 (PC) reporter system to detect *Mycobacterium tuberculosis* DNA in 2017³². The luciferase was designed to

be split half and fused with two separate dCas9 proteins. After PCR amplification, two dCas9 proteins bind to the closely located sequence in target DNA leading the reconstitution of luciferase and bioluminescence signal in the presence of APT and O₂.

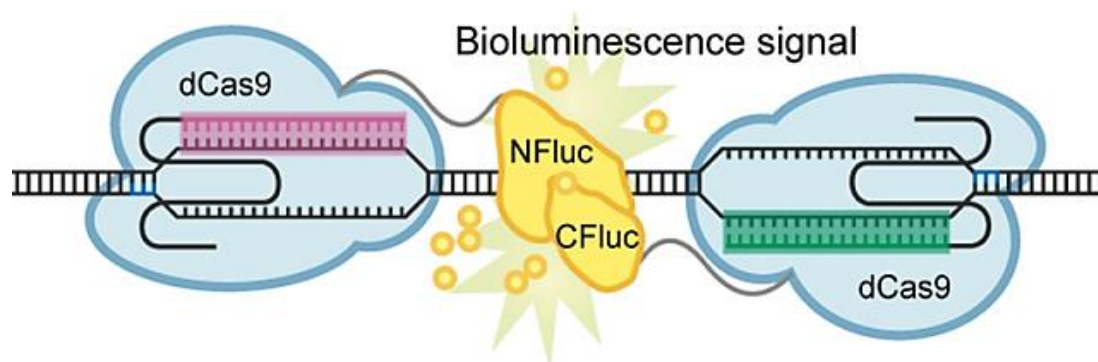


Figure 1.7 RNA-guided featured DNA detection by the paired dCas9 (PC) reporter method³² (Reprinted with permission from ref³², Copyright 2017, American Chemical Society).

Lingyun Zhu's group developed the first CRISPR/dCas9 based miRNAs detection platform called Rolling Circle Amplification (RCA)-CRISPR-split-Horseradish peroxidase (HRP) (RCH) system³³. The N and C terminal halves of the HRP protein (split-HRP-N and split-HRP-C) were separately fused with two separate dCas9 proteins. After miRNA target induced RCA, the proximal binding of two dCas9 to RCA products induced the dimerization of split-HRP-N and split-HRP-C and activated the colorimetric change of TMB.

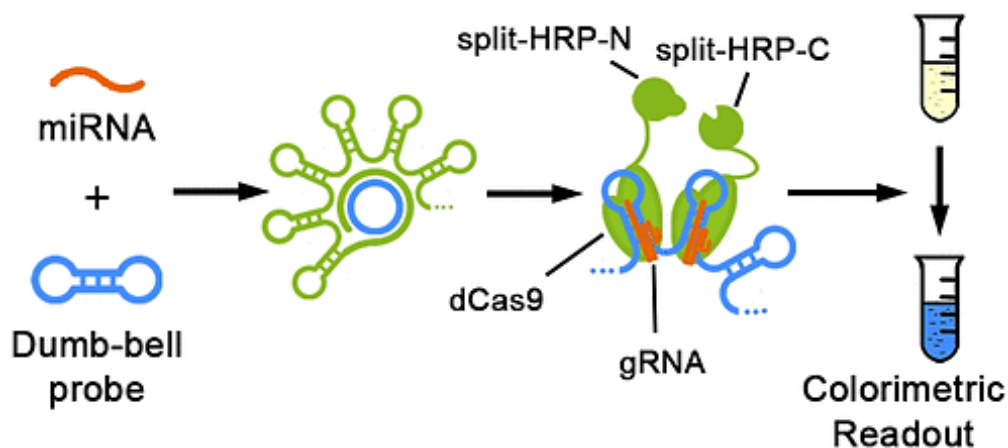


Figure 1.8 Overview of the Rolling Circle Amplification (RCA)-CRISPR-split-Horseradish peroxidase (HRP) (RCH) method³³ (Reprinted with permission from ref ³³, Copyright 2018, American Chemical Society).

Recently, another kind of dCas9 assay based on target binding induces electrical change was developed. In 2019, Kiana Aran's group successfully detected unamplified target DNA via CRISPR–Chip within 15 min, with a sensitivity of 1.7 fM³⁴. The dCas9 assembled with a target-specific sgRNA was immobilized on the graphene surface, selectively bind with the target sequence and unzipped the double helix structure. This target induced structure change modulated the surface electrical characteristics resulting in an electrical signal change.

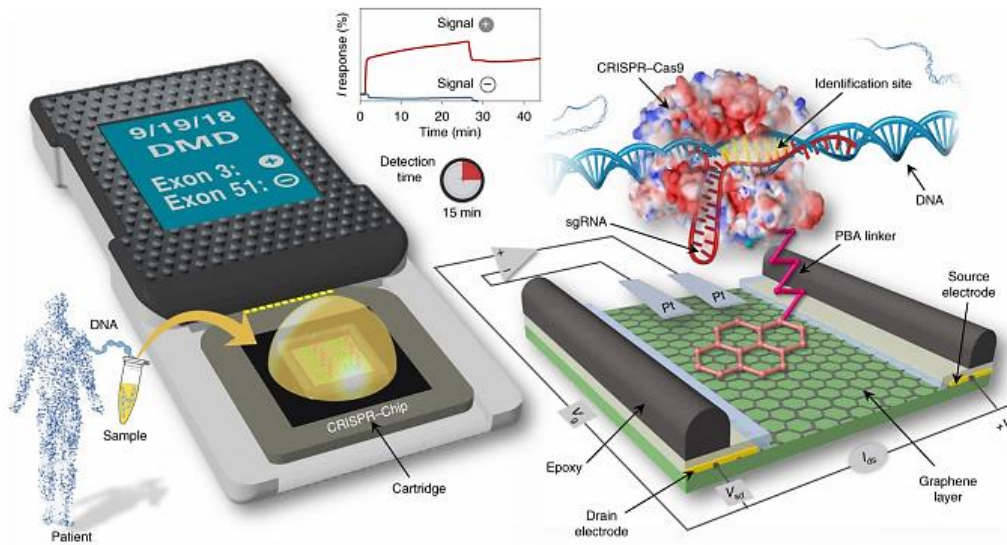


Figure 1.9 CRISPR–Chip for unamplified gene detection³⁴ (Reprinted with permission from ref³⁴, Copyright 2019, Springer Nature).

1.3.2 Cas12 Effector-based CRISPR/Cas Biosensing Systems

Cas12a (also called Cpf1) is RNA guided DNase, which can target both ssDNA and dsDNA followed by a collateral cleavage activity to indistinguishably degrade nearby trans-ssDNA^{19,23}. In 2018, Jennifer A. Doudna’s group developed Cas12a nucleic acid detection method named DNA endonuclease targeted CRISPR trans reporter (DETECTR)³⁵. DETECTR enriched target sequence by recombinase polymerase amplification (RPA), utilized Cas12a protein to detect crRNA-dependent DNA target and activated the nonspecific ssDNA trans cleavage activity to degrade fluorophore quencher (FQ)-labeled ssDNA reporters. Degradation of the DNA reporters separated fluorophores from quenchers resulting in increasing fluorescent signal. DETECTR has been used to detect human papillomavirus (HPV) and discriminate genotypes between HPV16 and HPV18 in patient samples.

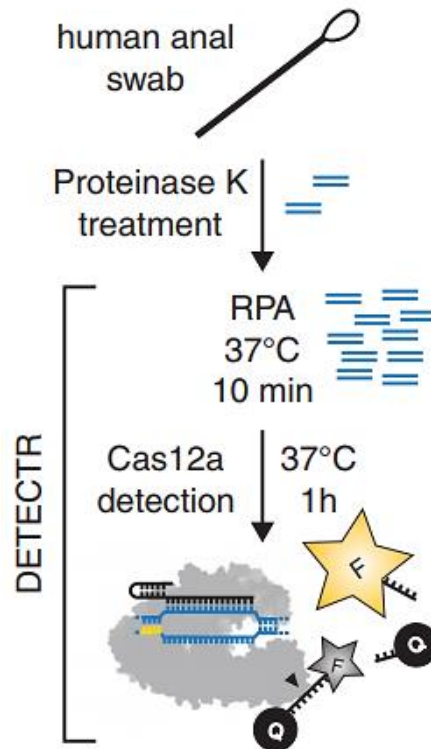


Figure 1.10 DNA endonuclease targeted CRISPR trans reporter (DETECTR) system³⁵ (Reprinted with permission from ref³⁵, Copyright 2018, American Association for the Advancement of Science).

During the same period, Jin Wang’s group developed a similar detection platform named one-Hour Low-cost Multipurpose highly Efficient System (HOLMES)³⁶. Instead of utilizing isothermal RPA in DETECTR, HOLEMES used PCR to amplify target sequence and the PAM sequence was designed as primers during PCR amplification. Cas12a proteins pre-assembled with target-specific crRNA were introduced to cleave amplified target products. After target detection, the quenched fluorescent ssDNA reporters were trans-cleaved, releasing the fluorescence signal. HOLMES has been used to not only detect DNA virus and RNA viruses like pseudorabies virus (PRV) and Japanese encephalitis virus (JEV) with attomolar

sensitivity but also distinguish human SNPs genotyping with single-based mismatch specificity.

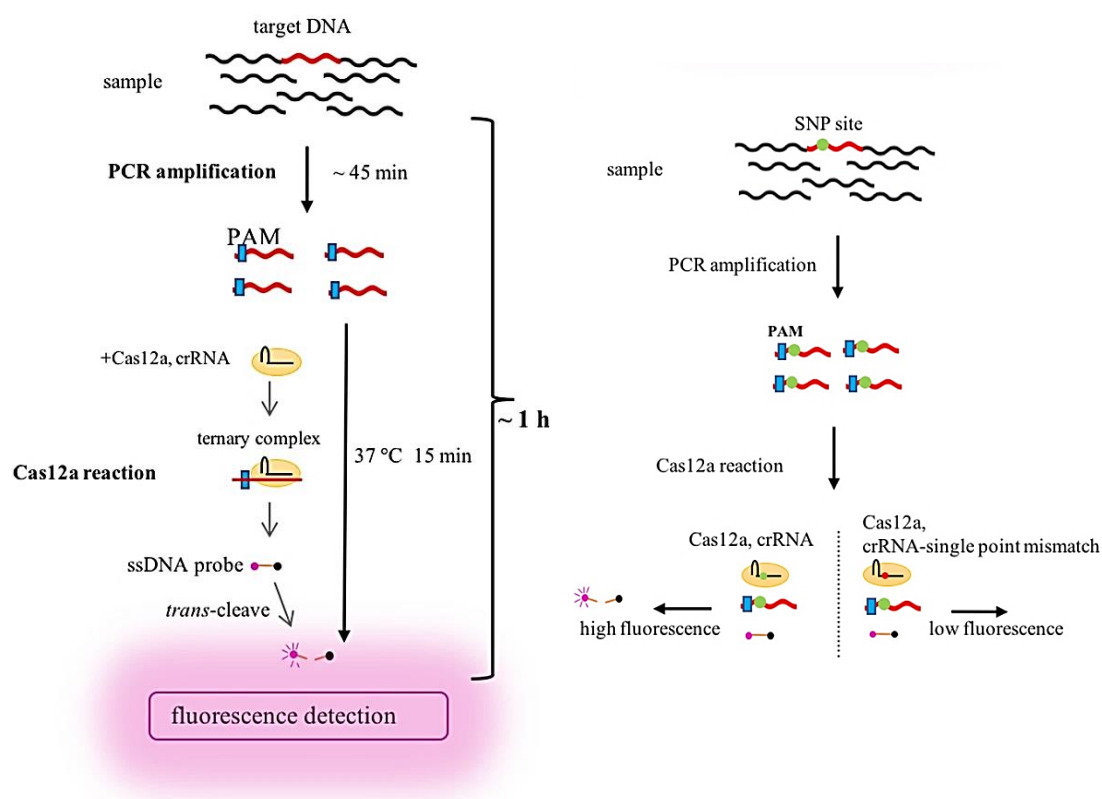


Figure 1.11 Schematic illustration of one-Hour Low-cost Multipurpose highly Efficient System (HOLMES) for DNA detection and SNP genotyping³⁶ (Reprinted with permission from ref³⁶, Copyright 2018, Springer Nature).

One year later, Jin Wang's employed thermophilic Cas12b proteins to create an updated version of HOLMES (HOLMESv2)^{37,38}. Compared with Cas12a, Cas12b has a wider range of reaction temperature (30-60°C); therefore, Cas12b nucleic acid detection can be combined with isothermal amplification methods, such as loop-mediated isothermal amplification (LAMP, reaction temperature of 60–65 °C), to construct one-pot nucleic acid detection system. HOLMESv2 could qualitatively evaluate nucleic acid samples with a one-step system combined with isothermal LAMP

amplification. HOLMESv2 also was applied for the detection of single nucleotide polymorphism (SNP) and DNA methylation.

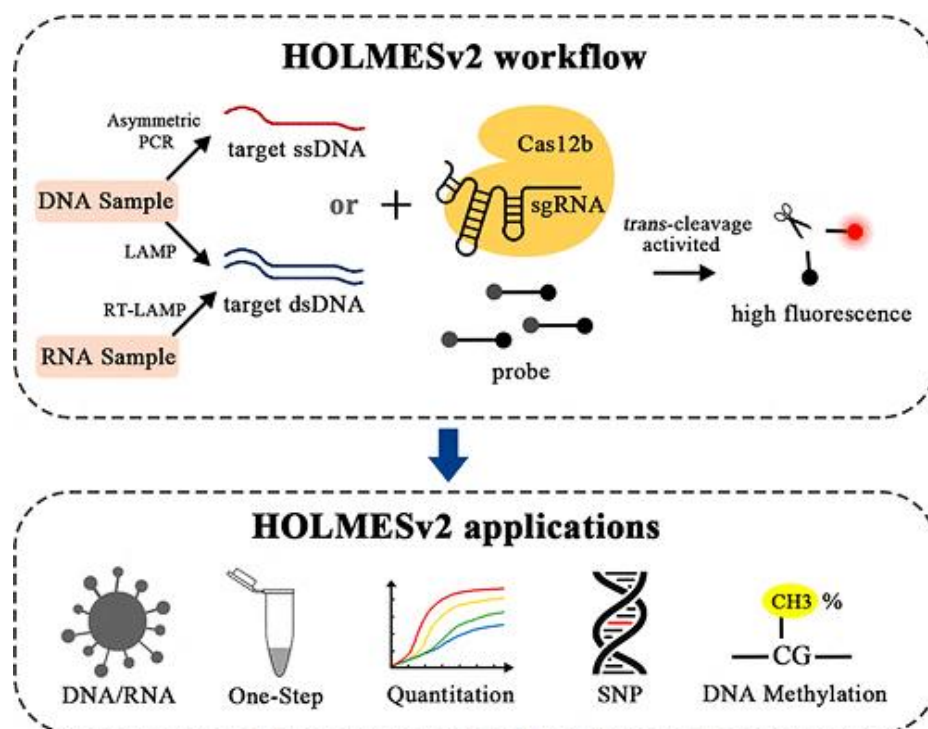


Figure 1.12 Schematic workflow and applications of one-Hour Low-cost Multipurpose highly Efficient System version 2 (HOLMESv2)³⁸ (Reprinted with permission from ref ³⁸, Copyright 2019, American Chemical Society).

In 2019, Dai and colleagues created a portable Cas12a based electrochemical biosensor (E-CRISPR)³⁹. After Cas12a detected their nucleic acid targets under the guidance of crRNA and activated trans-cleavage activity, the modified ssDNA reporter with methylene blue electrochemical tag attached to the sensor surface was cleavage by Cas12a proteins, decreasing the level of the electrochemical signal. E-CRISPR achieved picomolar (pM) sensitivity for detecting viral nucleic acids, including human papillomavirus 16 (HPV-16) and parvovirus B19 (PB-19). Moreover, an aptamer-based E-CRISPR cascade was designed for TGF- β 1 protein

detection in clinical samples. Hence, E-CRISPR can be potentially developed as portable and cost-effective diagnostic systems for various nucleic acids and proteins at the POC setting.

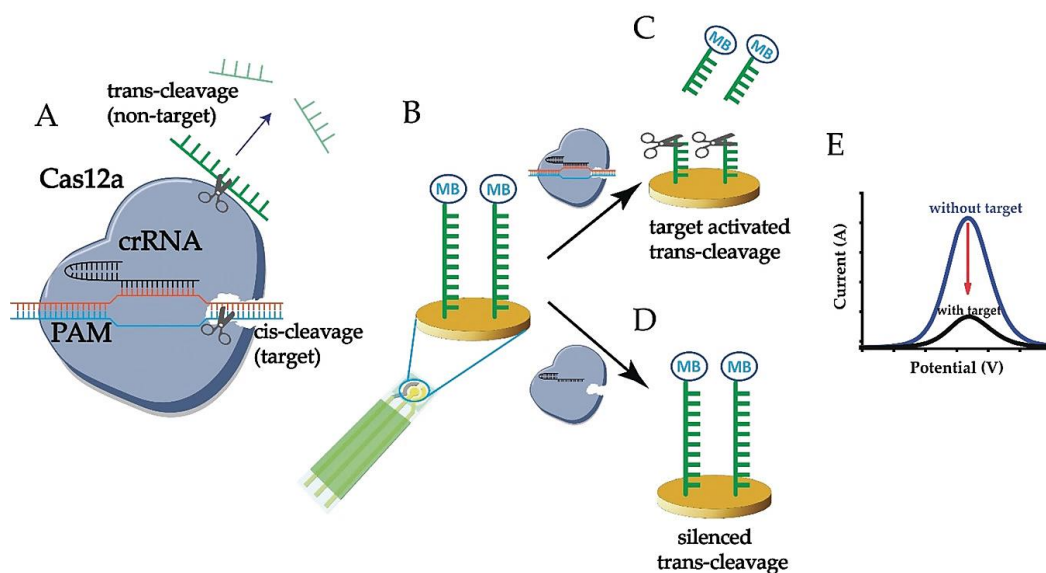


Figure 1.13 Schematic of E-CRISPR for nucleic acid detection³⁹ (Reprinted with permission from ref³⁹, Copyright 2019, Wiley-VCH Verlag GmbH & Co. KGaA, Weinheim).

1.3.3 Cas14 Effector-based CRISPR/Cas Biosensing Systems

In 2018, Jennifer Doudna's group firstly characterized Cas14 proteins, a highly diverse family of RNA-guided Cas protein to target and cleave single-stranded DNA (ssDNA) or single-stranded RNA (ssRNA) without PAM sequence restriction²¹. Compared with Cas12 proteins with larger size (950 to 1400 amino acids), Cas14 proteins are exceptionally compact (400 to 700 amino acids). Despite their small size, Cas14 shows lower tolerance to base-pair mismatches between crRNA and nucleic acid target. Cas14 exhibits collateral activity like Cas12a and degrades any nearby ssDNA after target recognition. Their properties make Cas14 potential in the development of

CRISPR-based biosensors. By deploying Cas14 in the DETECTR platform, single nucleotide polymorphisms (SNPs) in the human HERC2 gene were detected²¹.

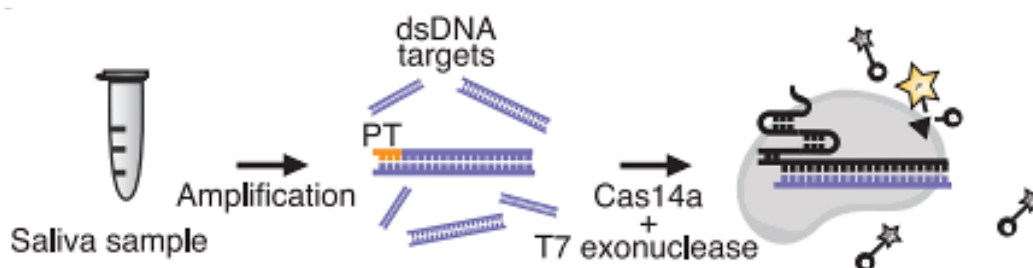


Figure 1.14 Diagram of Cas14-DETECTR strategy²¹ (Reprinted with permission from ref²¹, Copyright 2018, American Association for the Advancement of Science).

1.3.4 Cas13 Effector-based CRISPR/Cas Biosensing Systems

Cas13a is an RNA-guided RNase to detect and cleave single-stranded RNA (ssRNA) target followed by a collateral activity that indiscriminately cleaves nearby ssRNA after target recognition^{20, 22, 40}. By utilizing this collateral activity, Feng Zhang's group developed a CRISPR/Cas13a based nucleic acid biosensing system, called Specific High-Sensitivity Enzymatic Reporter UnLOCKing (SHERLOCK) method, to detect both DNA and RNA targets with single-base mismatch specificity and attomolar (aM) sensitivity⁴¹. Target DNA or RNA was amplified and converted to RNA by recombinase polymerase amplification (RPA) or reverse transcription-RPA (RT-RPA) and then followed by T7 transcription. Cas13a pre-assembled with crRNA was applied to detect the amplified target and activated collateral activity to degrade ssRNA report releasing fluorescence signal. The utilities of SHERLOCK were confirmed to detect

Zika virus, dengue virus, various pathogenic bacteria, SNPs and low-frequency cancer mutation in cell-free DNA⁴¹.

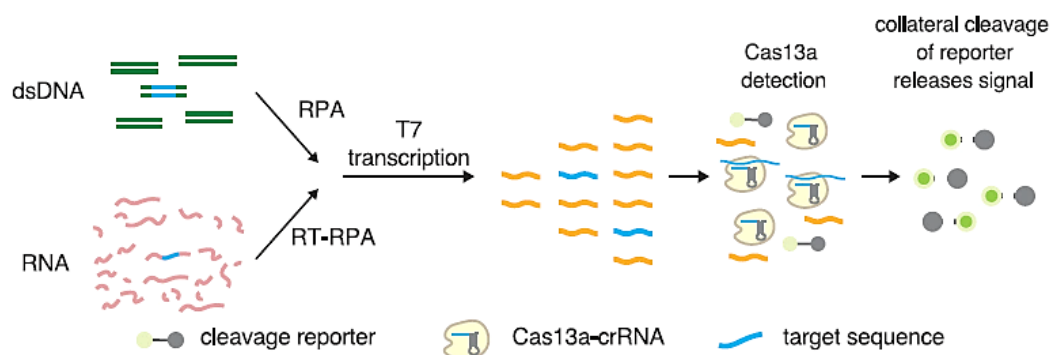


Figure 1.15 Schematic of Specific High-Sensitivity Enzymatic Reporter UnLOCKing (SHERLOCK)⁴¹ (Reprinted with permission from ref⁴¹, Copyright 2017, American Association for the Advancement of Science).

However, SHERLOCK only provides qualitative information for a single target sequence. To improve SHERLOCK for multiplexed quantitative detection, Feng Zhang's group later developed the updated version of SHERLOCK platform, SHERLOCKv2. SHERLOCKv2 employed 4 Cas proteins (LwaCas13a, PsmCas13b, CcaCas13b, and AsCas12a) with different cleavage preference on dinucleotide reporters to detect multiple targets simultaneously in 4 different fluorescent channels⁴². After target recognition, these 4 kinds of Cas proteins degraded corresponding dinucleotide reporters (LwaCas13a to AU, PsmCas13b to GA, CcaCas13b to UC, AsCas12a to ssDNA), and released fluorescence signal in TEX (LwaCas13a), FAM(PsmCas13b), Cy5(CcaCas13b), and HEX(AsCas12a) channels. To increase the accuracy of quantitative measurement, low concentration primers were used to make reactions unsaturated so that signal intensity was strongly correlated with target concentration. By adding Csm6 proteins, a 3.5-fold increased sensitivity was observed

for Cas13 quantitative measurement, because the Cas13 (LwaCas13a and PsmCas13b) collateral activity-induced cleavage product contained 2',3'-cyclic phosphate ends which can efficiently activate Csm6 to cleavage reporter probe further amplifying released signal. Also, a portable paper-based lateral flow readout based on a FAM-biotin reporter with anti-FAM antibody and gold nanoparticle was developed for detection on commercial lateral flow strips.

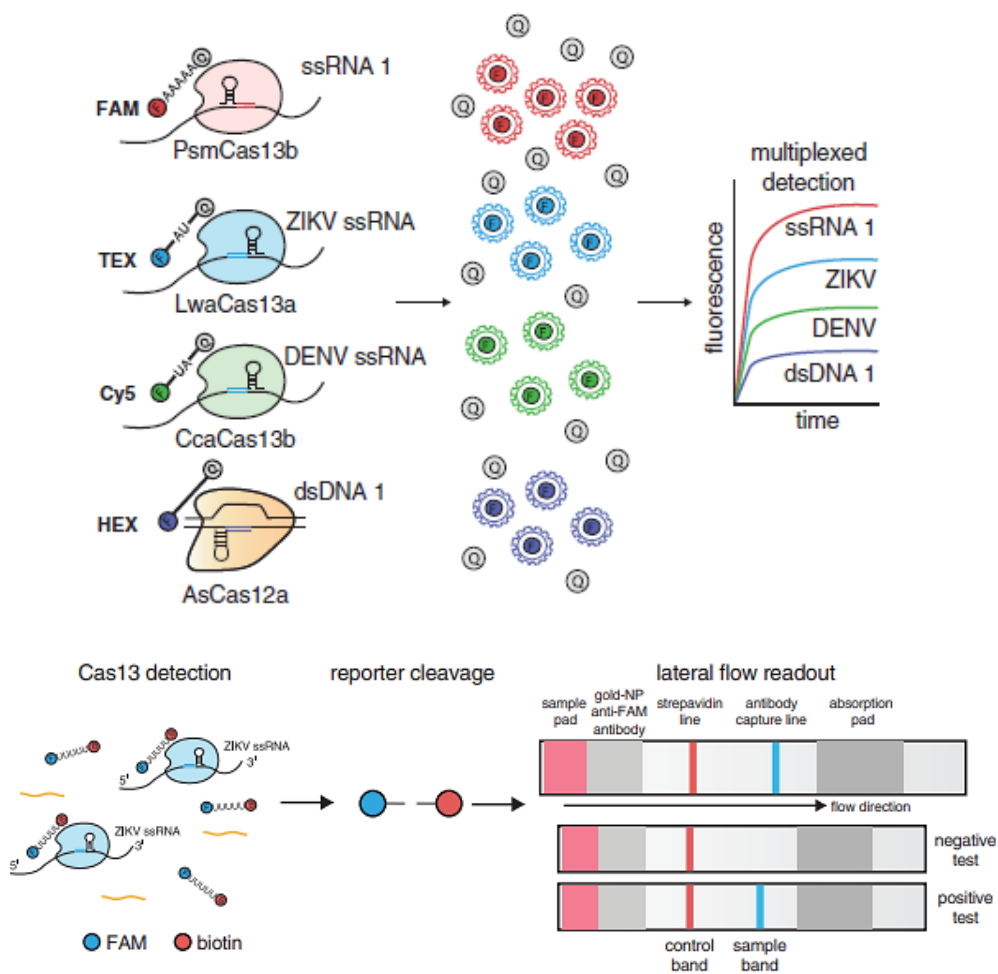


Figure 1.16 Schematic of Specific High-Sensitivity Enzymatic Reporter UnLOCKing version 2 (SHERLOCKv2)⁴² (Reprinted with permission from ref ⁴², Copyright 2018, American Association for the Advancement of Science).

1.4 Present Challenges and Conclusions

These introduced CRISPR/Cas-based methods have successfully demonstrated the promising potential of CRISPR/Cas systems to be developed as highly sensitive, specific, rapid and cost-efficient nucleic acid biosensing systems. By coupling with various amplification strategies (NASBA¹¹, EXARP³⁰, SDA³¹, PCR^{27,36}, RCA³³, RPA⁴¹ and LAMP³⁷), the detection sensitivity can be greatly improved into at least fM or mostly aM concentration. Also, with an increasing number of Cas protein candidates with diverse characteristic have been discovered, their biosensing applications have been widely applied to broadly diverse fields, including detections of DNA, RNA, SNP, DNA methylation and genotype; moreover, the specificity has been improved from Cas9 to Cas12 and Cas14 based systems. Most recently, the quantitative and multiplex capabilities of CRISPR/Cas biosensing systems have been achieved. Result readouts producing visual colorimetric signal observed by naked eyes or fluorescence signal detected by portable readers have facilitated the POC diagnostic applications of CRISPR/Cas-based biosensing systems.

In the future, with the demanding applications of CRISPR/Cas-based biosensing systems for various diagnostic purposes, it is critical to further modify or improve the performance of CRISPR/Cas biosensing systems, or even develop new systems. The CRISPR/Cas based biosensing systems may still have several challenges to overcome before they can be applied as practicable diagnostic tools. Challenges can be from either CRISPR/Cas systems or the integrated techniques to assist and enhance the detective performance. CRISPR/Cas systems can be further improved by highly specific Cas

proteins, reduced PAM sequence requirements and simplified guide RNA optimizations. Nowadays, identifying and investigating novel CRISPR/Cas systems are the hottest research topics in the biological field, especially for the Cas proteins with low tolerance to nucleotide mismatches or collateral properties to assist biosensing.

Moreover, the sequence limitations caused by PAM sequence and guide RNA are the main challenges for Cas protein detection. CRISPR effectors such as Cas9 and Cas12 detect dsDNA in a PAM-dependent manner (PAM sequence NGG for SpCas9 and TTTN for LbCas12). Although the PAM site requirements are easily met in the long sequence detection, such as pathogen detection, it is hard to satisfy for SNP distinguish and short sequence detection, which may limit the wider applications of CRISPR/Cas biosensing systems.

Currently, careful design and time-consuming optimization of guide RNA are required to minimize off-target effects before practical applications. Long stranded guide RNA provides a strong driving force for Cas protein to recognize nucleic acid target; however, the energy loss of few base pair mismatch can be overcome by this strong driving force inducing off-target effect. Although short stranded guide RNA can enhance the detective performance of SNP, it can reduce the specificity to recognize the nucleic acid target in the genome sequence, especially there are similar sequences in the same genome. In silico design and optimization can be growing trends to assist and accelerate the experimental processes of guide RNA.

Except for CRISPR/CAS systems, external techniques can be added in to facilitate biosensing applications, including sample preparation, signal amplification and signal

reporting. Most existing sample preparation methods require extensive sample manipulation and expensive machinery, which cannot satisfy the demand for field-deployable and rapid detections. Recently developed HUDSON (heating unextracted diagnostic samples to obliterate nucleases) protocol can inspire the development of field-deployable and instrument-free sample treatment. HUDSON utilizes heat and chemical reductions to extract viral nucleic acid directly from clinical samples via a one-pot procedure without extra extraction and separation steps⁴³. In the future, various sample pre-treatment strategies are in demand to fully support the sample sources from distinct environments and organisms.

The low sensitivity problem of Cas protein detection alone has been solved by coupling with various amplification techniques, including conventional PCR and isothermal amplification strategies. To achieve high sensitivity, amplification techniques usually provide enormous amplification force to make reactions saturated, but losing the quantitative information corresponding to relative sample concentration. Moreover, for most techniques, the amplification steps are separated from detection because of distinct reaction temperature, inapplicable buffer or interactive enzymes; therefore, future CRISPR/Cas biosensing systems can be optimized as one-pot systems integrating amplification and detection steps to eliminate possible contamination and manual operations during solution transfer.

Most current CRISPR/Cas biosensing systems rely on fluorescent, colorimetric and electrical signal readouts. Fluorescent signals are most widely used as result readouts; however, fluorescence reader is required to detect signals and computer is used to

interpreter results, which may increase assay cost. In the future, portable fluorescence reader can be developed to reduce economic cost and simplify the assay process. Colorimetric readouts directly observed by naked eyes are suitable strategies for POC diagnostics and field-deployable detections. Nevertheless, the naked eye only can justify qualitative result based on color change providing yes or no answer.

To conclude, the applications of CRISPR/Cas biosensing systems have been confirmed for detecting various targets, including DNA, RNA and proteins, leading the next-generation revolution in the molecular diagnostics field. This revolution has been driven by solving the challenges in existing systems, that CRISPR/Cas biosensing systems eventually are transformed into a novel, efficient and cost-efficient approaches for versatile applications in a variety of complex conditions.

Chapter 2: A Universal Plasmonic CRISPR Cas12a Assay for Field-Deployable Viral Diagnostics

Contribution Statement

The content of this chapter was modified from the published paper: Naked-eye Detection of Grapevine Red-blotch Viral Infection Using a Plasmonic CRISPR Cas12a assay.⁴⁴ Reprinted with the permission from Li, Y.; Mansour, H.; Wang, T.; Poojari, S.; Li, F., Naked-eye Detection of Grapevine Red-blotch Viral Infection Using a Plasmonic CRISPR Cas12a assay. *Analytical Chemistry*, **2019**, 91, 18, 11510–11513. Copyright 2019, American Chemical Society.

Yongya Li is the first author of this paper. Yongya Li conducted all experiment parts, including proof of principle, condition optimizations and sample validations. Hayam Mansour provided PCR amplicons for synthesized plasmid DNA. Tony Wang and Sudarsana Poojari collected grapevine samples infected by red blotch virus, extracted viral DNA and provided PCR amplified DNA products. This work was supervised by Dr. Feng Li.

2.1 Introduction

Viral infections are major threats to human health and agricultural crop productions worldwide. The pandemic severe acute respiratory syndrome (SARS),⁴⁵ Zika infection,⁴⁶ and H1N1 influenza⁴⁷ are only a few of many examples of life-threatening infections in the modern world. Other emerging viral infections, such as hepatitis B

virus (HBV),⁴⁸ are less catastrophic but may still cause severe adverse health outcomes, public fear, and economic loss. Meanwhile, the profitability and sustainability of agricultural crop productions, such as grape and wine industry, are also currently threatened by viral infections. For example, the emerging grapevine red-blotch virus (GRBV) infection is estimated to cause economic losses in the range of \$2,231 to \$68,548 (USD) per hectare per year.⁴⁹ The effective treatment and management of both human and crop infections require field-deployable diagnostics capable of rapid detection and routine monitoring of disease outbreaks in infrastructure-constrained settings. Standard nucleic-acid-based viral diagnostic tests, such as quantitative polymerase chain reaction (qPCR), are very sensitive and rapidly adaptable but are performed predominately at centralized laboratories because of the need for expensive and bulky instrumentation. Miniaturization of qPCR into field-deployable viral diagnostics requires not only portable thermal cyclers or isothermal PCR-alternatives but also visual, colorimetric readouts to facilitate the rapid signal generation and decision making.^{50,51} Herein, we introduce a simple, rapid, and universal color developer for amplicons produced by PCR or isothermal nucleic acid amplification. This color developer is created via the integration of target-induced CRISPR-Cas12a single-stranded DNase (ssDNase) activation and color transition mediated by plasmonic gold nanoparticles (AuNPs).

Plasmonic nanoparticles, such as AuNPs, have long been attractive colorimetric readout for nucleic acid testing (NAT).⁵² Despite the successful uses in the sensitive detection of single-stranded DNA (ssDNA)⁵³⁻⁵⁶ or RNA targets (e.g. NanoFlare

assays),^{57,58} the specific detection of point mutations,^{53,59} and lateral flow assays,⁶⁰ direct color development for double-stranded DNA (dsDNA) amplicons produced by PCR or many isothermal nucleic acid amplification techniques, such loop-mediated isothermal amplification (LAMP) remains an unmet challenge. As such, deployment of plasmonic nanoparticles to standard NAT requires significant modification of assay protocols (e.g. asymmetric PCR) to produce ssDNA or extensive modification of primers (e.g. lateral flow assays). We reason that this challenge can be addressed by the recent finding that RNA-guided DNA binding of CRISPR-associated enzyme Cas12a could unleash its indiscriminate ssDNA cleavage activity.^{61,62} Using this principle, dsDNA amplicons produced by PCR or LAMP can be detected directly in a sequence-specific manner without the need for any modification to primers or assay protocols. Here, by combining CRISPR-Cas12a-mediated target recognition with AuNP-induced color development, we successfully demonstrated the colorimetric, visual detection GRBV in grapevine samples and HBV in human serum samples with attomolar sensitivity.

2.2 Materials and Methods

2.2.1 Materials

Solutions of 20-nm gold nanoparticles (AuNPs), TWEEN 20, 10 × phosphate buffer saline (PBS), magnesium chloride (MgCl₂), and sodium chloride (NaCl) were purchased from Sigma (Oakville, ON, Canada). EnGen Lba Cas12a (Cpf1), WarmStart LAMP Kit, OneTaq Master Mix, and 10 × NEBuffer™ 2.1 Buffer were purchased from

New England Biolabs Ltd. (Whitby, ON, Canada). NANOpure H₂O (> 18.0 MΩ), purified using an Ultrapure Mili-Q water system, was used for all experiments. All DNA samples and the guide RNAs were purchased from Integrated DNA Technologies (Coralville, IA) and purified using high-performance liquid chromatography. The DNA sequences and modifications are outlined in Table S1.

2.2.2 DNA Sequence and Modifications

DNA name	Sequence (5'-to-3')
1.AuNP-immobilized Arm DNA sequence for A-AuNPs & B-AuNPs and Linker	
Arm-A	HS-AAA AAA AAA ACC TCA CCA CCA ACA C
Arm-B	HS-AAA AAA AAA ACA CAC ACA CTC ACA C
S	GTG TGA GTG TGT GTG GTG TTG GTG GTG AGG
2.Random Targets Detection	
NTS-35	GCT TGT GGC CG <u>TTTA CGT CGC CGT CCA GCT CGA CC</u>
TS-35	<u>GGT CGA GCT GGA CGG CGA CG TAAA</u> CGG CCA CAA GC
crRNA	UAA UUU CUA CUA AGU GUA GAU CGT CGC CGT CCA GCT CGA CC
3.Grapevine Red Blotch-associated Virus Detection after PCR Amplification	
NTS _{GRBV}	GCA CGT CGG CGA CAT CTC TGG GCT TTG TGA TAT TGG GGT GAT AGG AAT GAG ACG ATA TGG TGA TGT CAA AGT GT <u>TTTG GAT TGC GAA TAG CCT GTC GT T TTT TGA AGA</u> TGA GCA AGG CGT GTA GGT GTG G
TS _{GRBV}	C CAC ACC TAC ACG CCT TGC TCA TCT TCA AAA <u>AAC GAC</u> <u>AGG CTA TTC GCA ATC CAAA</u> AC ACT TTG ACA TCA CCA TAT CGT CTC ATT CCT ATC ACC CCAATA TCA CAA AGC CCA

	GAG ATG TCG CCG ACG TGC
Primer-D	GCA CGT CGG YGA CAT CTC TG
Primer-R	CCA CAC CTA CAC GCC TTG C
crRNA _{GRBV}	UAA UUU CUA CUA AGU GUA GAU GAT TGC GAA TAG CCT GTC GT
4.Hepatitis B Virus Detection after LAMP Amplification	
TS _{HBV}	TCC TCA CAA TAC CGC AGA GTC TAG ACT CGT GGT GGA CTT CTC TCA ATT TTC TAG <u>GGG GAA CTA CCG TGT GTC</u> <u>TTG GCC AAAA</u> TT CGC AGT CCC CAA CCT CCA ATC ACT CAC CAA CCT CTT GTC CTC CAA TTT G TC CTG GTT ATC GCT GGA TGT GTC TGC GGC GTT TTA TCA TCT TCC TCT TCA TCC TGC TGC
NTS _{HBV}	GCA GCA GGA TGA AGA GGA AGA TGA TAA AAC GCC GCA GAC ACA TCC AGC GAT AAC CAG GAC AAATTG GAG GAC AAG AGG TTG GTG AGT GAT TGG AGG TTG GGG ACT GCG AA TTTT <u>GGC CAA GAC ACA CGG TAG TTC CCC</u> CTA GAA AAT TGA GAG AAG TCC ACC ACG AGT CTA GAC TCT GCG GTA TTG TGA GGA
crRNA _{HBV}	UAA UUU CUA CUA AGU GUA GAU GC CAA GAC ACA CGG TAG TTC
F3 _{HBV}	TCC TCA CAA TAC CGC AGA GT
B3 _{HBV}	GCA GCA GGA TGA AGA GGA AT
F1P _{HBV}	GTT GGG GAC TGC GAA TTT TGG CTT TTT AGA CTC GTG GTG GAC TTC T
B1P _{HBV}	TCA CTC ACC AAC CTC TTG TCC TTT TTA AAA CGC CGC AGA CAC AT
LF _{HBV}	GGT AGT TCC CCC TAG AAA ATT GAG
LB _{HBV}	AAT TTG TCC TGG TTA TCG CTG G

* For all dsDNA target sequence, the bolded region is PAM sequence (TTTN).

* For all dsDNA target sequence, the underlined region is the sequence detected by

crRNA-Cas12a complexes.

2.2.3 Experimental Procedures

2.2.3.1 Preparation of DNA Functionalized AuNPs

DNA functionalized AuNPs were prepared by conjugating thiolated DNA oligonucleotides onto the 20nm AuNPs according to our previously established protocol.^[1] Briefly, 40 μ L of 5 μ M DNA-A or DNA-B were mixed with 500 μ L of 20nm AuNPs (1.16 nM), respectively. The mixture was incubated at room temperature for 12hrs and slowly mixed with 16.5 μ L of 3 M NaCl solution, followed by 10s of sonication. The salt ageing process was repeated five times with 1h interval. The mixture was then centrifuged at 13,500 rpm for 30 min to separate the DNA-AuNPs from excess thiolated DNA oligonucleotides. The supernatant was discarded and DNA-AuNPs were washed with 1 mL 1 \times PBS buffer (ph 7.4) containing 0.01% TWEEN 20. The washing steps were repeated for four times. The DNA-AuNPs was finally dispersed in PBS buffer at 2 nM final concentration and stored at 4°C.

2.2.3.2 Plasmonic Assay Protocol

For a typical plasmonic assay, a reaction solution containing 1 nM AuNP-A, 1 nM AuNP-B and 30 nM S or Cas12a degraded S was incubated at 50°C for 15 minutes and then cooled to the room temperature. The color of the solution was recorded as an image and the absorbance of which was then scanned from 450 nm to 700 nm at a resolution of 1 nm using a Multimode Microplate reader (SpectraMax i3, Molecular Devices).

2.2.3.3 Plasmonic CRISPR-Cas12a Assay

For typical plasmonic CRISPR-Cas12a assays, a reaction mixture containing 30 nM Cas12a, 30 nM of gRNA, 60 nM ssDNA substrate (S), and varying concentrations of target DNA, PCR amplicon, or LAMP amplicon was incubated at 37°C for 30 min. followed by an enzyme denaturation step. 10 µL of this reaction mixture was then mixed with an equal volume of AuNP solution and then tested using the plasmonic assay protocol outlined above.

2.2.3.4 PCR Protocol

For a typical PCR reaction, 2 µL target DNA was added to a reaction mixture containing Taq 2× Master Mix, 200 nM reverse primer, 200 nM forward primer to a final volume of 25 µL. PCR was then performed for 35 cycles in a BioRad T100 Thermal Cycler.

2.2.3.5 Polyacrylamide Gel Electrophoresis (PAGE)

A 5-µL solution containing PCR or LAMP amplicons was mixed with loading buffer and then loaded onto 6% PAGE gel. A voltage of 110 V was applied for driving the electrophoresis. After electrophoresis, the gel was stained with Ethidium Bromide and imaged using Gel Doc XR+ Imager System (BioRad).

2.2.3.6 Grapevine Sample Collection and DNA Extraction

Field grapevine samples representing both white- (Vidal Blanc) and red-fruited

(Baco Noir) interspecific hybrids as well as white- (Chardonnay and Riesling) and red-fruited (Cabernet Franc and Cabernet Sauvignon) *V. vinifera* cvs. were collected from commercial vineyard blocks in the Niagara region during September in 2018. Total nucleic acids (TNAs) were extracted from individual petiole samples (four petioles/vine) using a previously reported method. 3,4 Briefly, samples extracts were prepared using 250 mg of petiole tissue with the aid of semi-automated HOMEX 6 homogenizer (BIOREBA AG, Switzerland) in 5 ml of extraction buffer and to isolate TNAs, 4µl of extraction buffer was added into 25µl of extraction solution with 1% 2-mercaptoethanol and denatured at 95°C for 10 min before using as a template for endpoint and ddPCR assays. TNAs isolated from healthy and infected leaf material from grapevines maintained at the phytotron facilities at Brock University were used as negative and positive controls, respectively.

2.2.3.7 Grapevine Sample Testing Using Droplet Digital PCR (ddPCR) and End-Point PCR

Each ddPCR reaction was prepared in a total volume of 20 µL, which consisted of 10 µL of 2 × QX200™ ddPCR™ EvaGreen Supermix (Bio-Rad, Mississauga, ON, Canada), 100nM each of 706D-F (5'-GCACGTCGGYGACATCTCTG-3') and 706D-R (5'-CCACACCTACACGCCTTGC-3') primers, 8µL RNase/DNase-free water and 1µL template DNA (30 ng/ µL). The ddPCR reaction mixture was added to 70 µL of QX200™ Droplet Generation Oil for EvaGreen (Bio-Rad, Mississauga, ON, Canada). Droplets were generated using QX200™ AutoDG™ Droplet Digital™ PCR System

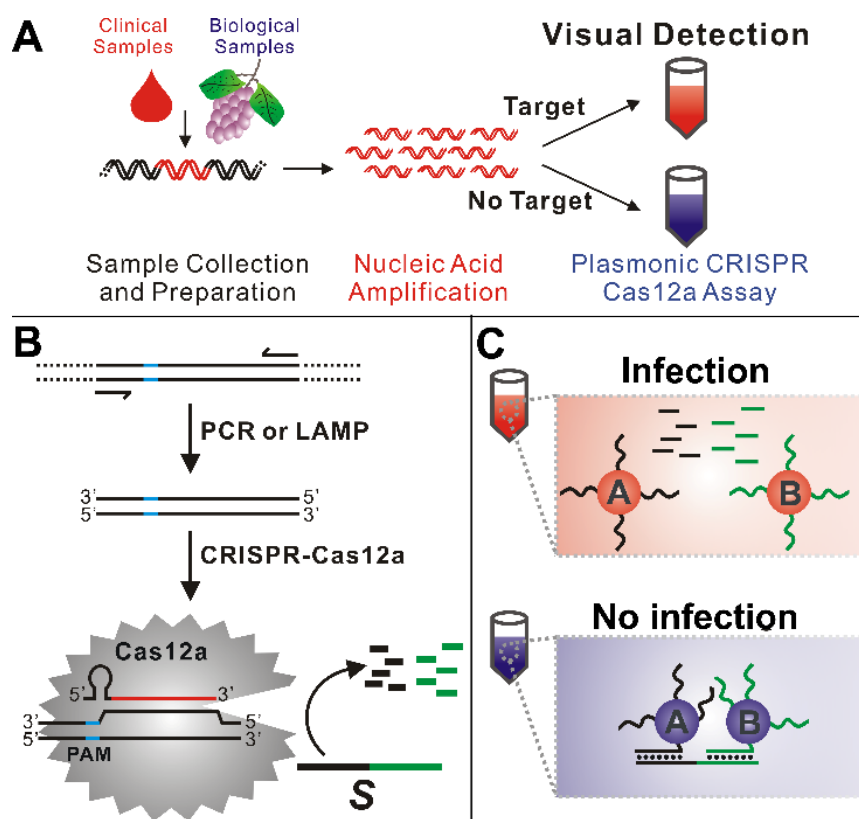
(Bio-Rad, Mississauga, ON, Canada). The PCR consisted of initial enzyme activation step at 95°C for 5 min and then 40 cycles of denaturation at 95°C for 30 sec and annealing and extension at 60°C for 1 min, followed by signal stabilization at 4°C for 5 min and 90°C for 5 min. The ramp rate of 2°C per second was followed during enzyme activation and denaturation steps. Three technical replicates were performed for all six samples tested as well as controls. The end-point PCR was performed in a C1000 Touch Thermal Cycler (Bio-Rad, Mississauga, ON, Canada) using primer sets (GVGF1 5' CTCGTCGCATTTGTAAGA-3') and GVGR1 (5'-ACTGACAAGGCC TACTACG-3') that were specific to partial ORF of V1 and V2 genes (256 to 821) of GRBV.

2.3 Result and Discussion

2.3.1 Assay Principle

Scheme 2.1 shows a typical workflow of plasmonic CRISPR Cas12a assay for analyzing genetic viral markers in a biological or clinical sample. Total nucleic acids are first extracted and amplified using standard extraction, PCR (or LAMP) protocols and virus-specific primers (Scheme 1A). The sequence-specific recognition is achieved through a CRISPR RNA (crRNA) that also recruits a Cas12a protein and unleashes its indiscriminative ssDNase activity (Scheme 1B). As a result, a single-stranded substrate (S) will be completely degraded in the presence of the genetic viral marker and subsequent PCR or LAMP amplicon. S also services as a linker that cross-links two DNA functionalized AuNPs, AuNP-A and AuNP-B, through hybridization (Scheme 1C). Upon cross-linking by S, the close proximity of AuNPs leads to a coupling of their

individual localized plasmon fields and thus a red-to-blue color transition. However, in the presence of the viral marker, S is degraded by Cas12a and the AuNP solution thus remains to be red. Therefore, by simply examining the color of the assay solution using naked eyes, we will be able to determine the presence (red) or absence (blue) of the viral infection. Moreover, as the sequence of S is independent of that of the target, the same plasmonic readout system can be generalized to any target of interest without any modification.



Scheme 2.1 Schematic illustration of the plasmonic CRISPR Cas12a assay for field-deployable nucleic acid testing. (A) Workflow for visual detection of viral infections in biological and clinical samples. (B) Target recognition using CRISPR-Cas12a and the activation of incriminating ssDNase activity. (C) Color development using plasmonic DNA functionalized AuNPs (Reprinted with permission from ref ⁴⁴, Copyright 2019, American Chemical Society).

2.3.2 Condition Optimizations

We first set out to examine the AuNP-based plasmonic readout. The concentration of the linker S is a critical parameter for resulting in a visual color change of the AuNP solution. In our experiments, we fixed the concentration of AuNP-A and AuNP-B to be 500 pM and varied the concentration of S from 0 to 50 nM. As shown in Figure 1A, the red-to-blue color transition occurs at 10 nM and saturated at 30 nM. We also measured the absorbance spectrum for each sample for the quantitative monitoring of the color change (Figure 1B). Consistent with the visual observation, the maximum absorbance λ_{\max} shifted from 526 nm to 560 nm when varying S from 0 nM to 50 nM (Figure 1C). As 30 nM is the minimal concentration resulting in a complete color transition, this concentration was used as an optimal parameter for the subsequent assay development.

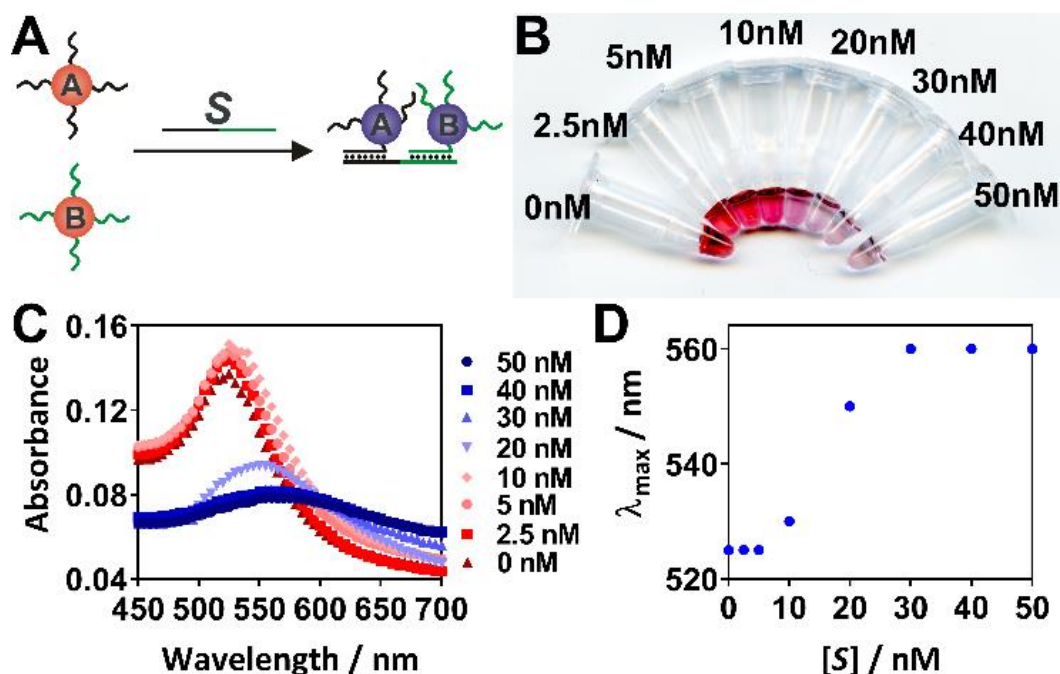


Figure 2.1 AuNP-based plasmonic readout. (A) Schematic illustration of the plasmonic readout using DNA-AuNPs. (B) Color transitions of AuNPs in the presence of varying concentrations of the linker S. (C) Absorbance spectra of DNA-AuNPs in the presence of S. (D) Maximum absorbance λ_{\max} as a function of varying concentrations of S (Reprinted with permission from ref ⁴⁴, Copyright 2019, American Chemical Society).

We next examined the compatibility of the plasmonic readout to the CRISPR Cas12a system. A 35-bp dsDNA containing a 5' TTTA protospacer-adjacent motif (PAM) was used as a model target. A crRNA was designed to contain 20-nt target-dependent sequence and an RNA scaffold to assist the detection of dsDNA target in a PAM-dependent manner. We found that crRNA and Cas12a interfered S for cross-linking AuNP-A and AuNP-B even in the absence of the target, which results in very little color change and shift of λ_{\max} (Figure 2.2A). A rapid increase of temperature followed by a slow cooldown step was found to restore the color change and promote the shift of λ_{\max} by 8 times (Figure 2.2B). By analyzing target dsDNA from 0.1 pM to 1 nM using the plasmonic CRISPR Cas12a assay with S fixed at 30 nM, we found a sharp color transition at 200 pM (Figure 2.3A), with a detection limit of 40 pM determined using the spectra shifts (Figure 2.3B). It is also possible to fine-tune the dynamic range of our assay by simply altering the concentration of S. As shown in Figure 2.3B, by using 60 nM S, the sharp color transition was found shifted to 800 pM.

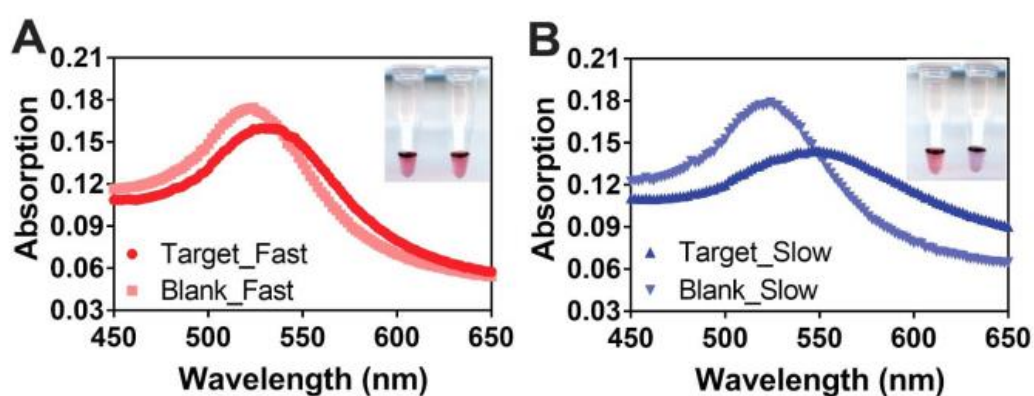


Figure 2.2. The optimal condition for the plasmonic assay in the presence of CRISPR Cas12a. The experiments were performed to confirm that the extended reaction time from 5 min (fast reaction, A) to 15 min (slow reaction, B) could facilitate the cross-linking of DNA-AuNPs in the presence of CRISPR Cas12a reagents. The wavelength shift of the maximal absorbance was increased from 4 nm (A) to 32 nm (B) (Reprinted

with permission from ref ⁴⁴, Copyright 2019, American Chemical Society).

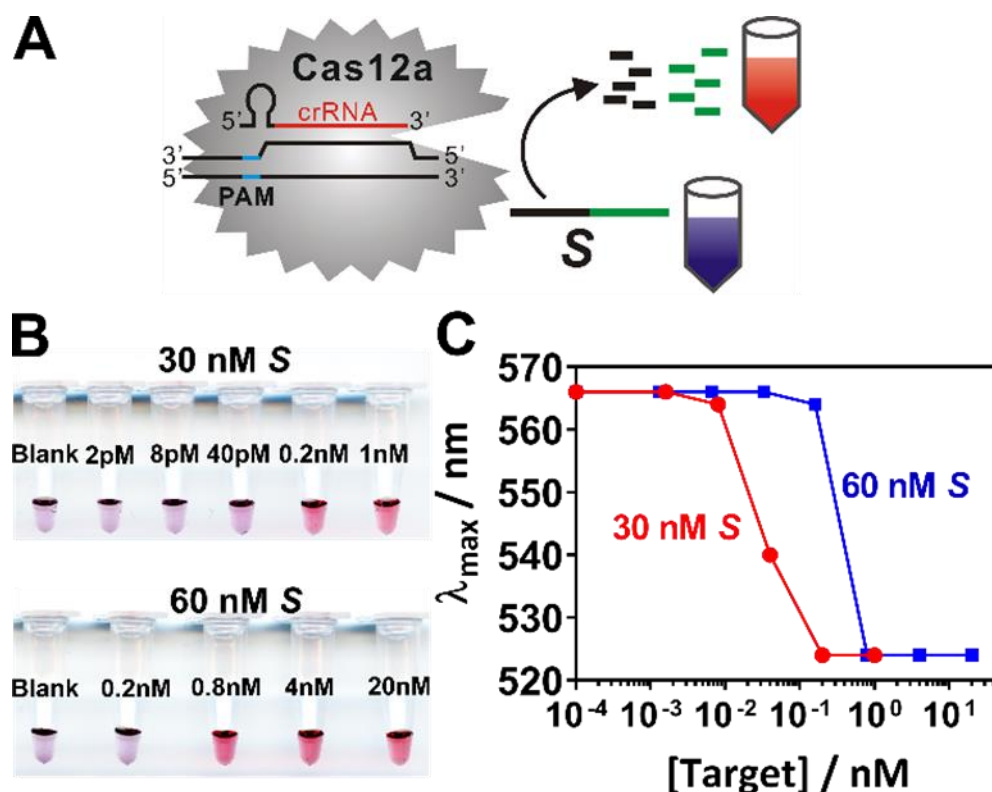


Figure 2.3 Plasmonic CRISPR Cas12a assay. (A) Schematic illustration of the plasmonic CRISPR Cas12a assay. (B) Images for visual detection of target dsDNA using plasmonic CRISPR Cas12a assays with 30 nM or 60 nM *S*. (C) Maximum absorbance λ_{\max} as a function of varying target concentrations. (Reprinted with permission from ref ⁴⁴, Copyright 2019, American Chemical Society).

2.3.3 Assay Validation for GRBV Infections Diagnostics

Having verified that the plasmonic readout is fully compatible with CRISPR Cas12a, we next challenged our plasmonic assay as a field-based diagnostic for GRBV infections in grapevine samples. Although GRBV infected red-berried cultivars of *Vitis* *Vinifera* L. can show characteristic symptoms on the mature leaves at post-véraison but such symptoms are less apparent on white-berried cultivars of *V. vinifera* and interspecific hybrids (Figure 2.4). In addition, symptoms of GRBV can also be confused with other viruses such as grapevine leafroll-associated viruses that infect grapevines.



Figure 2.4. Representative symptoms of grapevine red blotch virus infections on the leaves of redfruited (Cabernet Franc, left) and white-fruited (Chardonnay, right) *Vitis Vinifera*. The reddish-purple patches on the leaves coalesce into bloches covering the entire leaf surface in case of red-berried cultivars, Cabernet Franc (left), whereas on white fruited cultivar, Chardonnay, the symptoms are less apparent with yellowish discoloration of leaf edges and necrotic spots can be seen (Reprinted with permission from ref ⁴⁴, Copyright 2019, American Chemical Society).

We first verified our assay for the detection of PCR amplicons generated from a 130-bp synthetic DNA standard corresponding to a sub-genome of GRBV at a location from 2,753 nt to 2,882 nt of the reference genome (JQ901105).⁶³ To enable CRISPR Cas12a recognition, a crRNA was designed to target a 20-nt sequence right after a 5' TTTG PAM domain. We found that our plasmonic assay is fully compatible with PCR and clear red solutions were observed for targets with concentrations varying from 10 nM to 1 pM (Figure 2.6). A blue color was observed in the absence of the target (blank). Having observed this exciting result, we next challenged our assay using real GRBV samples collected from infected grapevine leaves (Figure 3B). As a comparison, we also extracted total DNA from leaves of healthy controls (Figure 3E). As shown in Figure 3C all three infected samples produce red colors upon PCR amplification and color development. By contrast, the two healthy controls produce blue colors, which

were the same as the blank (Figure 3F). All results were consistent with the standard polyacrylamide gel electrophoresis (PAGE) analyses (Figure 2.7). These results suggest that our assay is suitable for visual diagnosis of grapevine viral infections and holds the potential for field-based uses.

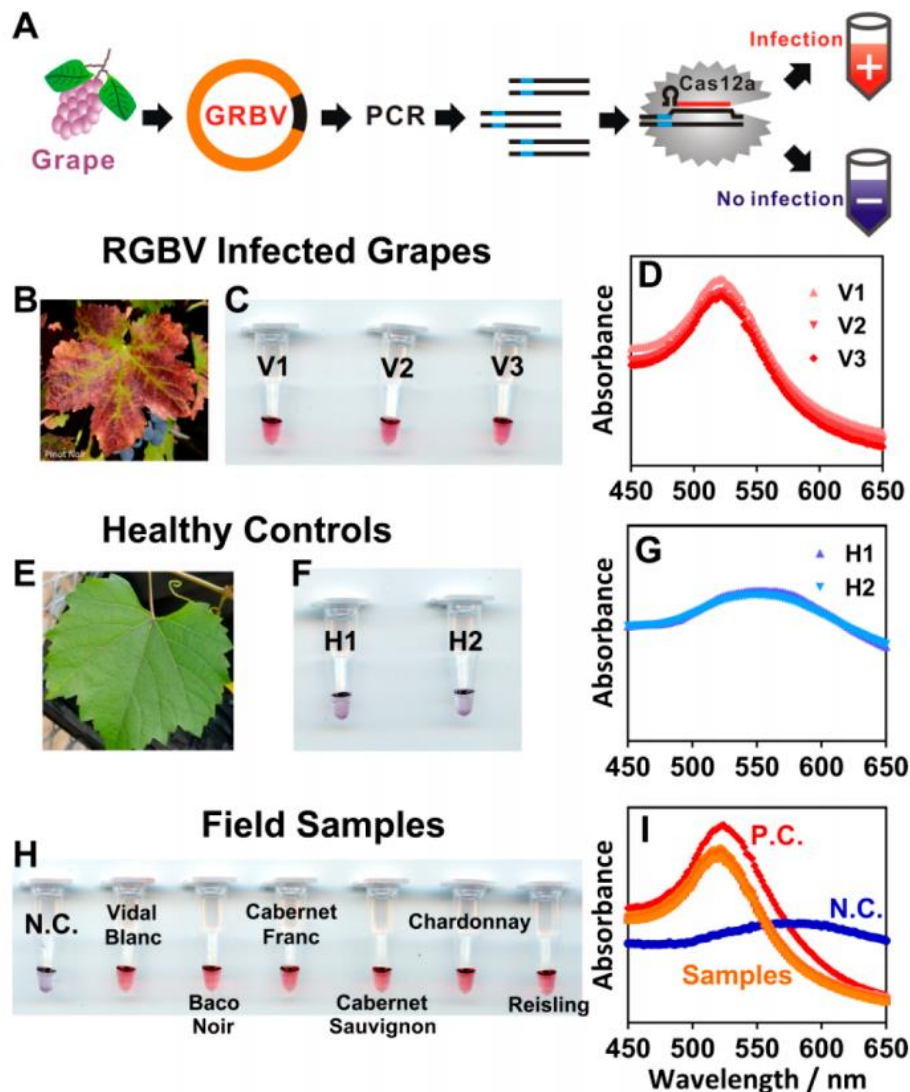


Figure 2.5 Visual detection of GRBV infection in grape samples using PCR and plasmonic CRISPR Cas12a assay. (A) Schematic illustration of the visual detection of GRBV infection in grape samples using PCR and plasmonic CRISPR Cas12a assay. (B) Image of a representative leaf of a GRBV infected grape. (C) Images for visual detection of GRBV infection for GRBV positive plants. (D) Absorbance spectra of GRBV positive tests. (E) Image of a representative leaf of a healthy grape. (F) Images for visual tests of healthy controls. (G) Absorbance spectra of GRBV negative tests in healthy controls. (H) Images for visual detection of GRBV infection for field samples. (I) Absorbance spectra of GRBV tests for field samples (Reprinted with permission

from ref ⁴⁴, Copyright 2019, American Chemical Society).

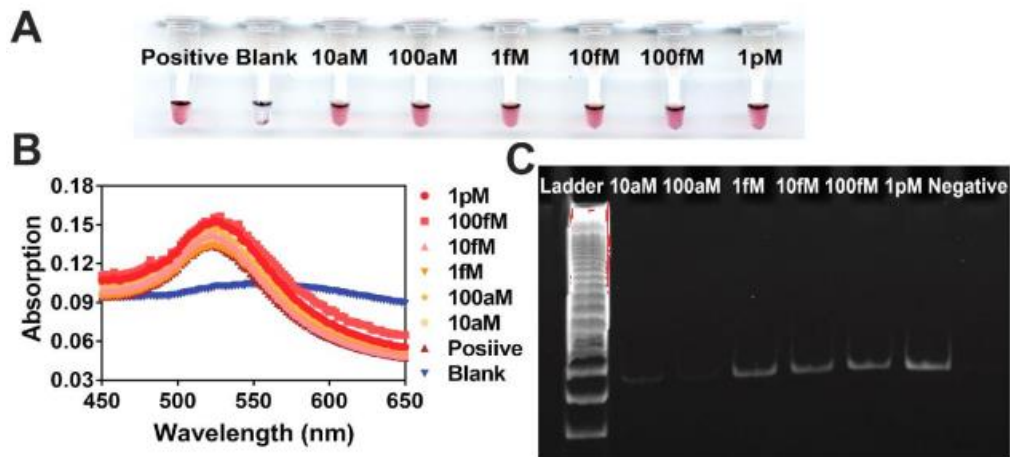


Figure 2.6 Visual analysis of PCR amplicons using the plasmonic CRISPR Cas12a assay. (A) Visual analysis of PCR amplicons of varying concentrations of synthetic DNA standards using the plasmonic CRISPR Cas12a assay. (B) Absorbance spectra of the colorimetric readout on the same samples shown in (A). (C) Parallel analyses of PCR amplicons using PAGE (Reprinted with permission from ref ⁴⁴, Copyright 2019, American Chemical Society).

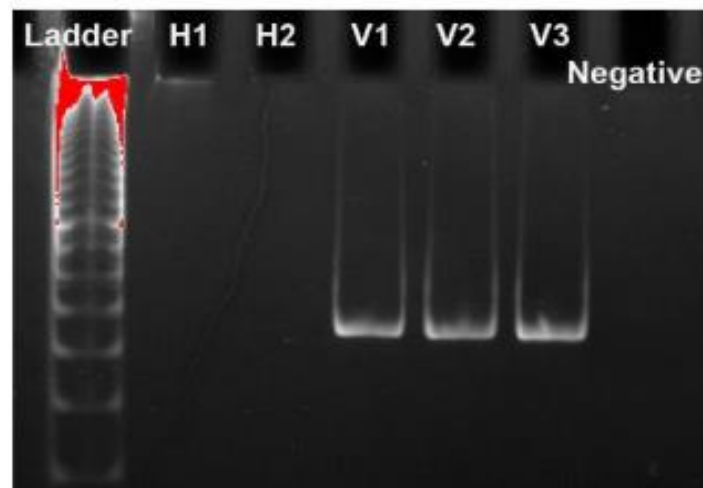


Figure 2.7 PAGE analysis of PCR amplicons of GRBV infected grape samples (V1, V2, V3) and health grape controls (H1, H2) (Reprinted with permission from ref ⁴⁴, Copyright 2019, American Chemical Society).

We finally challenged our assay for analysing real grapevine samples collected in field. Six grapevine samples representing both white- (Vidal blanc) and red-fruited (Baco Noir) interspecific hybrids as well as white- (Chardonnay and Riesling) and red-fruited (Cabernet Franc and Cabernet Sauvignon) *V. vinifera* cvs. were collected from commercial vineyard blocks in Niagara, Canada. Total nucleic acids were extracted from petiole samples. All six samples were found to be GRBV infected using our plasmonic assay, evidenced by the red-colored reaction solutions (Figure 3H). This result was further confirmed using standard PCR followed by PAGE analysis and droplet digital PCR (Figure 2.8). To test the robustness of assay for field applications, we also made a dilution series for each sample. As shown in Figure 2.9, we found that accurate diagnostic results could be obtained for samples subject to 2,000 to 10,000 dilutions, suggesting that our assay is highly robust, and can tolerant substantial DNA loss often occur during sample pre-treatment in field.

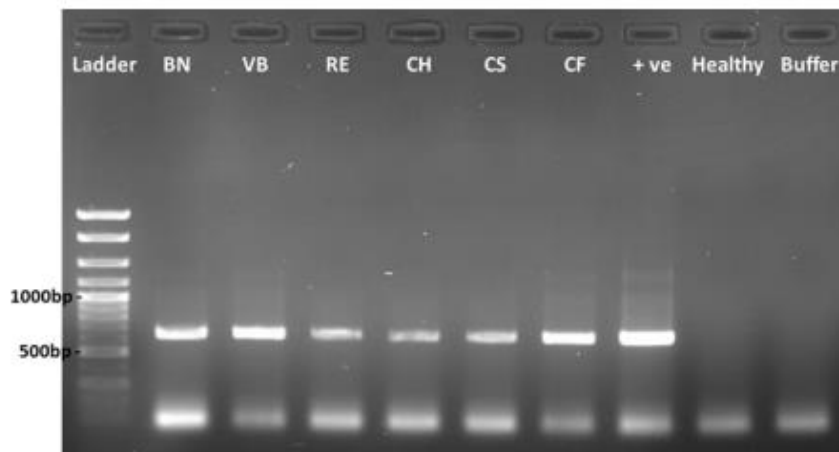


Figure 2.8 Detection of GRBV isolates by end-point PCR and electrophoresis. Gel Green (Biotium, USA) stained 1% agarose gel electrophoresis image of the PCR amplicons of grapevine red blotch virus (GRBV). Names of the 6 isolates along with controls were mentioned on the top of the gel in white and the size of the reference marker mentioned on the left in black. BN-Baco Noir; VB-Vidal Blanc; RE-Riesling;

CH- Chardonnay; CS- Cabernet Sauvignon; CF- Cabernet Franc (Reprinted with permission from ref⁴⁴, Copyright 2019, American Chemical Society).

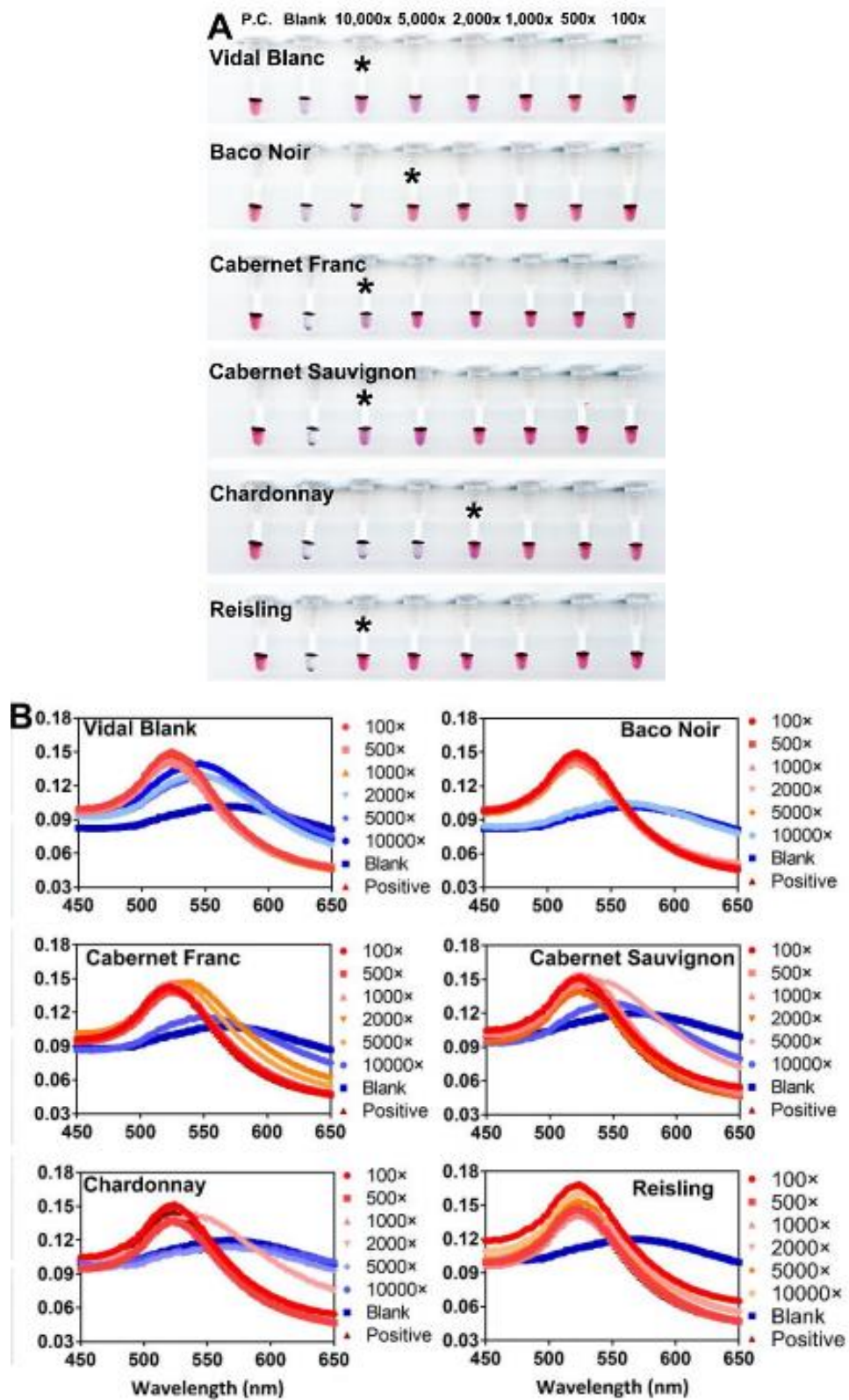


Figure 2.9 Visual detection of GRBV infected grapevine leaf samples using PCR and

plasmonic CRISPR Cas12a assay. (A) Visual detection of GRBV infected grapevine leaf samples with varying dilution factors using PCR and plasmonic CRISPR Cas12a assay. (B) Absorbance spectra of the colorimetric readout on the same samples shown in (A) (Reprinted with permission from ref ⁴⁴, Copyright 2019, American Chemical Society).

2.3.4 Assay Validation for HBV plasmids Detection

To move standard NAT from centralized laboratories to field, isothermal nucleic acid amplification techniques are often used as PCR alternatives. We finally verified the compatibility of our plasmonic assay to isothermal nucleic acid amplification. LAMP was chosen as a specific testbed because of its wide applications in field-based tests (Figure 4). A 1.3K-mer WT amplicon HBV plasmid was used as a model target.⁶⁴ A set of six primers were designed to amplify a 192-bp fragment of HBV S-gene containing a 5' TTTG PAM sequence.⁶⁵ A crRNA was designed corresponding to the 20 nt sequence adjacent to PAM. Upon LAMP amplification followed by the plasmonic CRISPR Cas12a assay, we were able to detect as low as 10 aM HBV plasmid by visualizing the red color of the solution or monitoring the spectra shifts). As LAMP is known to be a highly rugged amplification technique, we were able to perform a direct LAMP for HBV plasmid spiked in undiluted human serum samples (Figure 4B). Our plasmonic assay is fully compatible with the direct LAMP protocol, producing distinguishable color change (Figure 4C) or spectrum shift (Figure 4D) for as low as 10 aM HBV DNA. These results were further confirmed using standard PAGE analyses (Figure 4E). Collectively, these results suggest that our plasmonic CRISPR Cas12a assay is highly sensitive and versatile, which can be expanded to isothermal nucleic acid amplification systems without the need for changing the design of plasmonic

readout.

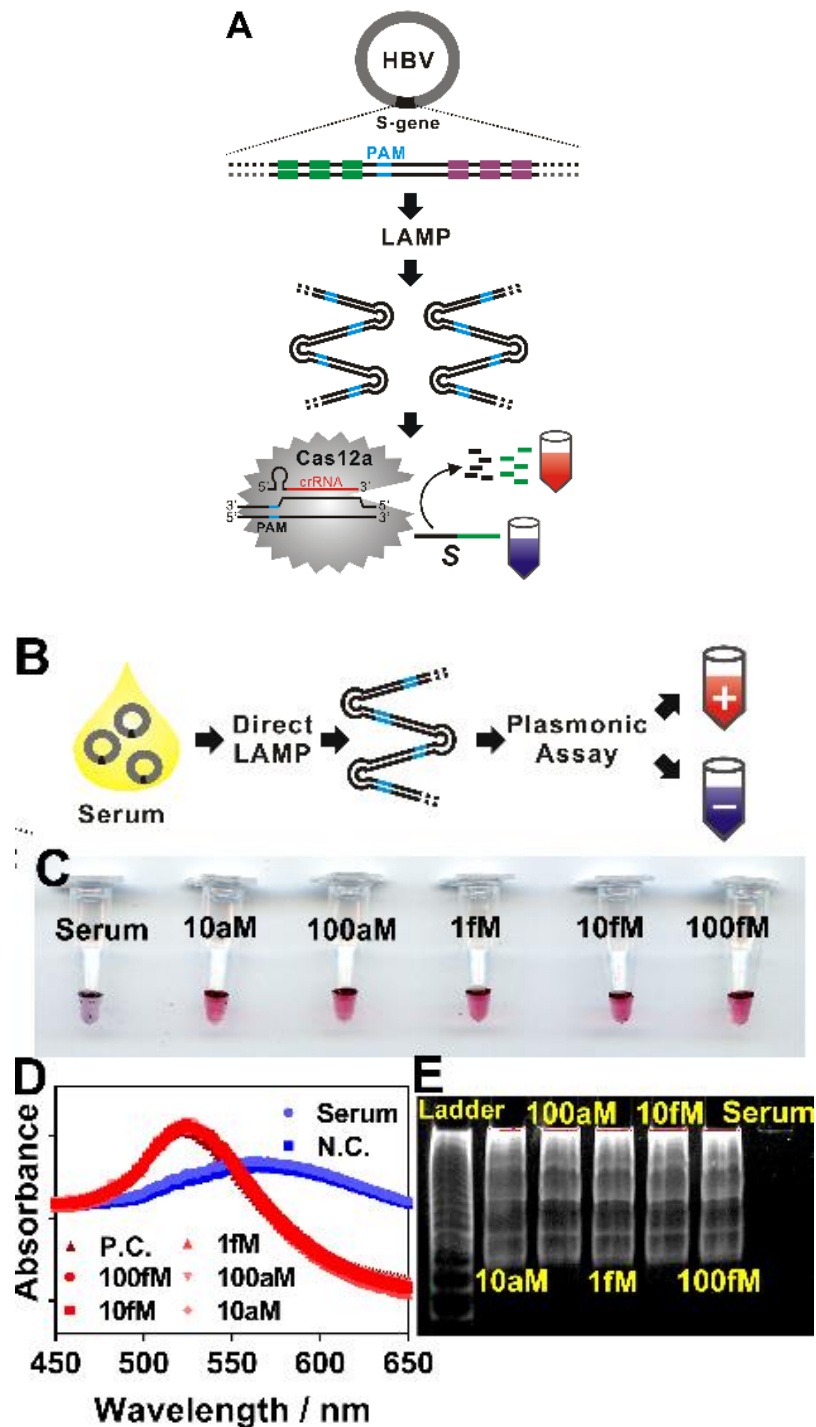


Figure 2.10 (A) Visual detection of HBV DNA using LAMP and plasmonic CRISPR Cas12a assay. HBV can be detected directly from undiluted human serum samples using a direct LAMP protocol (B). (C) Images for visual detection of HBV plasmids spiked in undiluted human serum samples using direct LAMP and plasmonic CRISPR Cas12a assays. (D) Absorbance spectra of serum samples containing varying concentrations of HBV DNA. (E) Parallel analyses of amplicons produced by direct

LAMP using polyacrylamide gel electrophoresis. (Reprinted with permission from ref ⁴⁴, Copyright 2019, American Chemical Society).

2.3 Conclusions

In conclusion, we have developed a novel plasmonic CRISPR Cas12a assay that generates visual, colorimetric readout for nucleic acid tests deployable to fields. One of the most valuable assets of our assay that it can act as a simple “add-on” color developer to the existing PCR or LAMP protocols and readily convert them into visual colorimetric tests. The sequence design of the plasmonic readout is independent of the target. Therefore, our assay can be expanded to diverse classes of genetic targets by simply switching a crRNA. We also successfully demonstrated the real-world applicability of our assay for analyzing grapevine viral infections from grape samples collected in field and HBV infections from pre-clinical samples. We anticipate that our plasmonic CRISPR Cas12a assay will also expand the toolbox and practical applicability of the current CRISPR-based diagnostics.

Chapter 3: A Universal Proximity CRISPR Cas12a Assay for Ultrasensitive Detection of Nucleic Acids and Proteins

Contribution Statement

The content of this chapter was modified from the published paper: A universal proximity CRISPR Cas12a assay for ultrasensitive detection of nucleic acids and proteins.⁶⁶ Reprinted with permission from Li, Y.; Mansour, H.; Tang, Y.; Li, F. A universal proximity CRISPR Cas12a assay for ultrasensitive detection of nucleic acids and proteins. *BioRxiv*, 2019, 734582, DOI: <https://doi.org/10.1101/734582>.

Hayam Mansour and Yongya Li contributed equally to this paper. Hayam Mansour optimized experimental conditions by utilizing synthesized DNA and antibody. Yongya Li assayed LAMP amplicons and protein samples. This work was jointly supervised by Dr. Yanan Tang and Dr. Feng Li. Yongya Li has permission from all authors to include figures and text from the paper in this chapter.

3.1 Introduction

Signal amplification is the key to the ultrasensitive detection of trace levels of biomarkers in biological and clinical samples. Recent advances in microbial clustered regularly interspaced short palindromic repeats (CRISPR) and CRISPR-associated (CRISPR-Cas) enzymes offer exciting opportunities for developing novel signal amplifiers that are both sensitive and specific.⁶⁷⁻⁷⁰ The RNA cleaving nuclease Cas13a was found to possess an indiscriminative ribonuclease activity upon the recognition of

specific RNA targets.⁶⁷ By combining the “collateral” cleavage of Cas13a with recombinase polymerase amplification (RPA), Zhang and co-workers introduced a series of specific high-sensitivity enzymatic reporter unlocking (SHERLOCK) techniques for the ultrasensitive detection of nucleic acids amenable for point-of-care (POC) applications.⁶⁸⁻⁷⁰ Doudna and coworkers have revealed the similar “collateral effect” of Cas12a, where single-stranded deoxyribonuclease (ssDNase) activities of Cas12a can be activated upon target recognition.⁷¹ A DNA endonuclease-targeted CRISPR trans reporter (DETECTR) system was further introduced via the integration with RPA, which enabled the detection of target DNA with attomolar sensitivity.⁷¹ So far, the detection of each specific genetic marker requires the design of a new CRISPR RNA (crRNA), which can be expensive and time-consuming. More importantly, it is not yet possible to expand such powerful detection systems to non-nucleic-acid targets, such as proteins. Herein, we introduce an alternative proximity CRISPR Cas12a strategy, where the target nucleic acid or protein will be translated into a universal pre-designed CRISPR-targetable DNA barcode in homogeneous solutions through a binding-induced primer extension reaction. By doing so, we can decouple the target recognition from the CRISPR Cas12a amplification and thus allow the broad adaptation to diverse DNA, RNA, and non-nucleic-acid targets.

3.2 Materials and Methods

3.2.1 Materials

EnGen Lba Cas12a (Cpf1), 10 × NEBuffer™ 2.1 Buffer, Klenow Fragment (3'→5' exo-), 10 × NEBuffer™ 2, Deoxynucleotide (dNTP) Solution Mix, nicking endonuclease (Nb.BbvCI) were purchased from New England Biolabs Ltd. (Whitby, ON, Canada). Anti-biotin antibodies were purchased from Thermo Fisher Scientific (Mississauga, ON, Canada). Human serum, magnesium chloride hexahydrate (MgCl₂·6H₂O), and 100×Tris-EDTA (TE, pH 7.4) buffer were purchased from Sigma-Aldrich (Mississauga, ON, Canada). NANOpure H₂O (> 18.0 MΩ), purified using an Ultrapure Mili-Q water system, was used for all experiments. All DNA samples and the guide RNAs were purchased from Integrated DNA Technologies (Coralville, IA) and purified using high-performance liquid chromatography.

3.2.2 DNA Sequences and Modifications

Name	Sequence (5'→3')
Nucleic Acid Detection	
P2 (Template)	GCT TGT GGC CG TTTA CGT CGC CGT CCA GCT CGA CCTCAGC CGT AGA TT GAC TCT GGC TTT-InvT
P1 (Primer)	ATC TCT CTG AAG TTT CTA CG
Blocking DNA	TTT TTT CGT AGA C
Target	AAA AGA TAA CAA GAA AGAC AAA GCC AGA GTC CTT CAG AGA GA TAC AGA AAC TCT AAT TCA
Protein Detection	
P2' (Template)	GCT TGT GGC CG TTTA CGT CGC CGT CCA GCT CGA CCTCAGC ATGCGTAGA TTT TTT TTT TTT TTT-Biotin

P1' (Primer)	Biotin-TTT TTT TTT TTT TTT TCTACG
CRISPR-Cas12a	
crRNA	UAA UUU CUA CUA AGU GUA GAU CGU CGC CGU CCA GCU CGA CC
Signal Reporter	FAM-TTA TT-Quencher

3.2.2 Experimental Procedures

3.2.3.1 Nucleic Acid Detection Using Proximity CRISPR Cas12a Assay

For a typical test, a 50 μ L reaction mixture contained 5 μ L of 100 nM P1, 5 μ L of 100 nM P2, 10 μ L of varying concentrations of the genetic target, 3.3 mmol of dNTPs, 5 units of Klenow Fragment and 0.5 unit of nicking endonuclease in 1X NEBuffer™ 2. The solution was incubated at 37 °C for 20 min. A 50 μ L enzyme solution which contains 30 nM of Cas12a, 30 nM of gRNA and 60 nM of the signal reporter in 1 \times NEBuffer™ 2.1 was added. Fluorescence was measured immediately after transferring the reaction mixture to a 96-well microplate and kept measuring every 30s for 2 hours at 37 °C using a SpectraMax i3 multi-mode microplate reader (Molecular Devices) with excitation/emission at 485/515 nm.

3.2.3.2 Proximity CRISPR Cas12a Assay with Blocking DNA

5 μ L of 100 nM P1, 5 μ L of 100 nM P2, 5 μ L of 200 nM blocking DNA and 10 μ L of the genetic target with varying concentrations were incubated at 37 °C for 30 min. This reaction mixture was then added with 3.3 mmol of dNTPs, 5 unit of Klenow Fragment and 0.5 unit of nicking endonuclease in 1X NEBuffer™ 2 to a final volume

of 50 μL . The solution was incubated at 37 $^{\circ}\text{C}$ for another 20 min. A 50 μL enzyme solution containing 30 nM of Cas12a, 30 nM of gRNA and 60 nM of the signal reporter in 1 \times NEBufferTM 2.1 was added. Fluorescence was measured immediately after transferring the reaction mixture to a 96-well microplate and kept measuring every 30s for 2 hours at 37 $^{\circ}\text{C}$.

3.2.3.3 Antibody Detection Using Proximity CRISPR Cas12a Assay

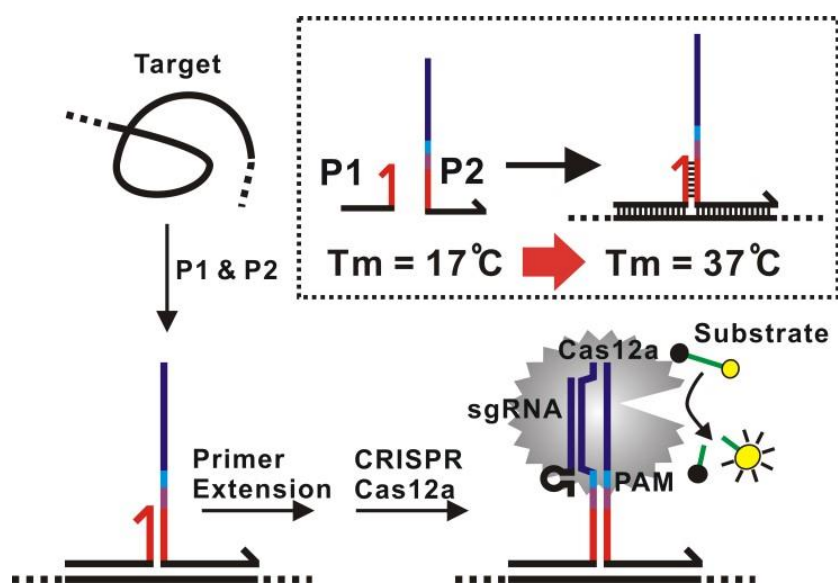
For a typical test, 5 μL of 100 nM P1', 5 μL of 100 nM P2' and 10 μL of varying concentrations of antibody were first mixed and incubated at 37 $^{\circ}\text{C}$ for 30 min. A 30 μL enzyme solution containing 3.3 mmol of dNTPs, 5 unit of DNA Polymerase (Klenow Fragment) and 0.5 unit of nicking endonuclease (Nb.BbvCI) in 1X NEBufferTM 2 was then added. The solution was incubated at 37 $^{\circ}\text{C}$ for 20 min. Another 50 μL enzyme solution containing 30 nM of Cas12a, 30 nM of gRNA and 60 nM of the signal reporter in 1 \times NEBufferTM 2.1 was added. Fluorescence was measured immediately after transferring the reaction mixture to a 96-well microplate and kept measuring every 30s for 2 hours at 37 $^{\circ}\text{C}$.

3.3 Results and Discussion

3.3.1 Assay Principle Illustration

As illustrated in Scheme 3.1, the CRISPR-targetable protospacer-adjacent motif (PAM) containing DNA barcode for activating Cas12a is generated in situ through a binding-induced primer extension reaction between P1 and P2. P2 is coded with a pre-

designed complementary sequence of the barcode. P1 and P2 contain a short 6-nt complementary sequence (red domains) with an estimated melting temperature (T_m) of 17 °C. Therefore, P1 and P2 do not hybridize under our assay condition (37 °C). However, in the presence of the target nucleic acid, P1 and P2 hybridize adjacently to the same target through complementary sequences (black domains), leading to the formation of a three-way junction with an estimated T_m of 37 °C (by NuPack). A primer extension reaction is then triggered to extend P1 to produce the DNA barcode which is recognized by the pre-designed crRNA. The ssDNase activity of Cas12a is then activated. A fluorescence turn-on assay can then be achieved by adding a short ssDNA substrate labelled with a fluorophore at the 5' end and a quencher at the 3' end, respectively. As the generation of the DNA barcode is quantitatively determined by the amount of the original target, the fluorescence signal can be used for target quantification.



Scheme 3.1 Schematic illustration of the proximity CRISPR Cas12a assay for the amplified detection of nucleic acids (Reprinted with permission from ref ⁶⁶).

3.3.2 Nucleic Acids Detections

We first set out to establish the proximity CRISPR Cas12a assay for the detection of nucleic acids (Figure 3.1). Upon the binding-induced primer extension followed by Cas12a cleavage, we were able to detect a synthetic target DNA with a limit of detection (LOD) at 10 pM (Figure 3.1B and Figure 3.1C). The LOD of our assay is comparable with that using direct crRNA recognition and Cas12a cleavage, suggesting that the binding-induced primer extension can effectively translate the detection of a target sequence to the production of the DNA barcode for the subsequent Cas12a-mediated amplification. To further push the LOD of our assay, we next integrated a nicking cleavage mechanism into the production of the DNA barcode (Figure 3.1A). Specifically, P2 was designed to contain a nicking recognition domain (purple) adjacent to PAM. Upon primer extension, a sequence that contains both the barcode for Cas12a activation and a nicking cleavage domain was generated. In the presence of a nicking endonuclease, the barcode was released through nicking cleavage and a new round of primer extension. As such, each target DNA could trigger the production of multiple single-stranded DNA barcodes that activate Cas12a ssDNase in a PAM independent manner and thus further amplify the detection signal.

As shown in Figure 3.1D, a drastic enhancement in sensitivity was observed when integrating the proximity CRISPR Cas12a amplification with nicking cleavage. We were able to improve the LOD by 100 times (Figure 3.1E and Figure 3.1G). Meanwhile, we also observed a high background, which makes it difficult to further distinguish targets of concentrations lower than 100 fM (Figure 3.1F).

To address this challenge, we further introduced a blocking DNA that competitively binds and consumes P1 (Figure 3.1H). This blocking strategy was found to effectively reduce the background, allowing the detection of target DNA with 1 fM LOD (Figure 3.1H and Figure 3.1I).

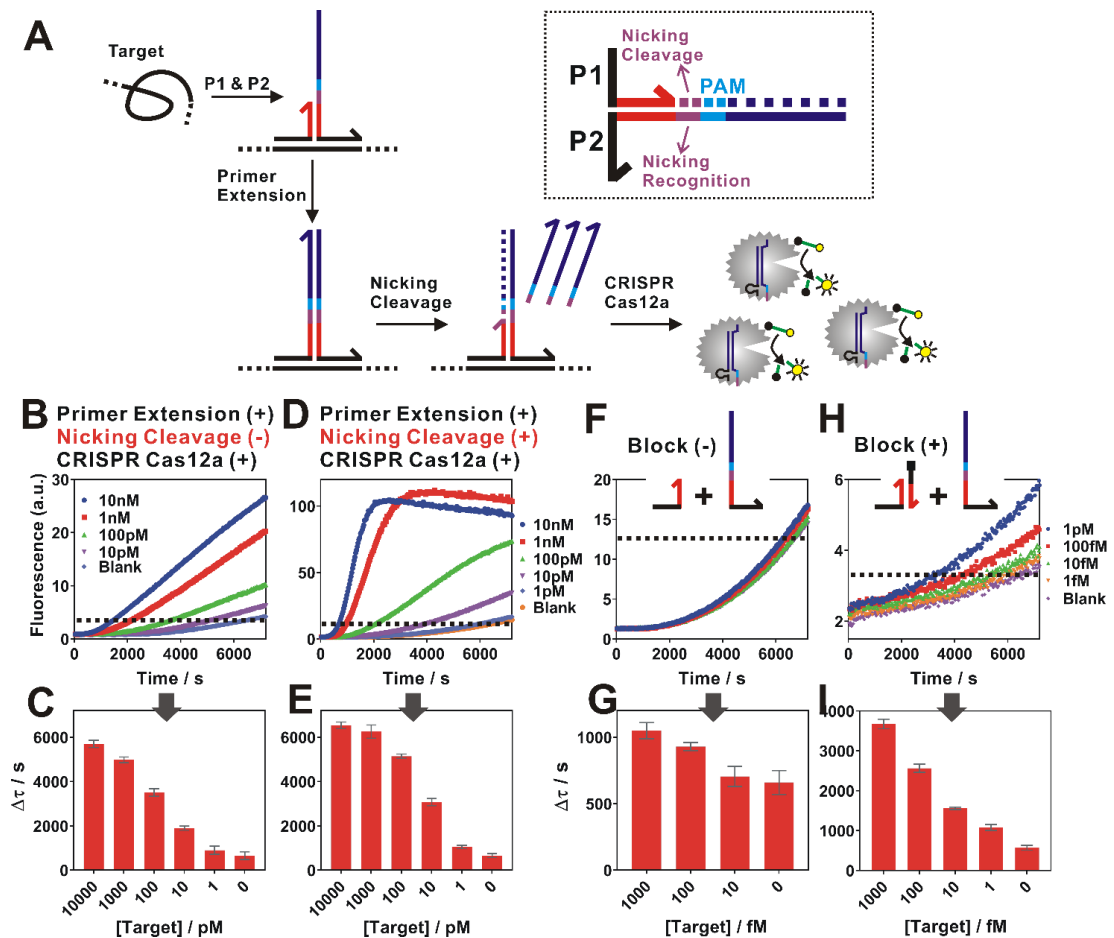


Figure 3.1 Proximity CRISPR Cas12a assay for the detection of nucleic acids. (A) Schematic illustration of the integration of proximity CRISPR Cas12a assay with nicking cleavage for further signal amplification. (B, C) Detection of a synthetic nucleic acid target using proximity primer extension followed by CRISPR Cas12a amplification. Once measuring the fluorescence increase in real-time (B), we set a threshold (dashed line) to determine the critical time τ , which is the minimal time to reach the threshold. A calibration curve was then established by plotting $\Delta\tau$ ($\Delta\tau = 7200s - \tau$) as a function of target concentrations (C). (D, E) Detection of nucleic acid target by integrating the proximity CRISPR Cas12a assay with nicking cleavage. (F, G) The detection of a target at concentrations from 1 fM to 1 pM using the proximity CRISPR Cas12a assay integrated with nicking cleavage. To further push the detection limit to lower target concentrations, a blocking DNA was introduced to suppress the background (H, I). Each error bar represents one standard deviation from triplicate analyses (Reprinted with permission from ref⁶⁶).

We next challenged practical applicability of this assay to real biological samples.

One advantage of the proximity recognition mechanism is that the target is not limited to DNA. RNA can also be recognized directly through proximity hybridization without the need for reverse transcription. Therefore, we demonstrated the use of this assay for profiling the temporal changes of IL-6 gene expression at the mRNA level during allergen-mediated mast cell activation (Figure 3.2). Rapid and quantified profiling of IL-6 gene expression during allergic reactions holds great potential for understanding and diagnosing diseases such as mastocytosis, anaphylaxis, and asthma.

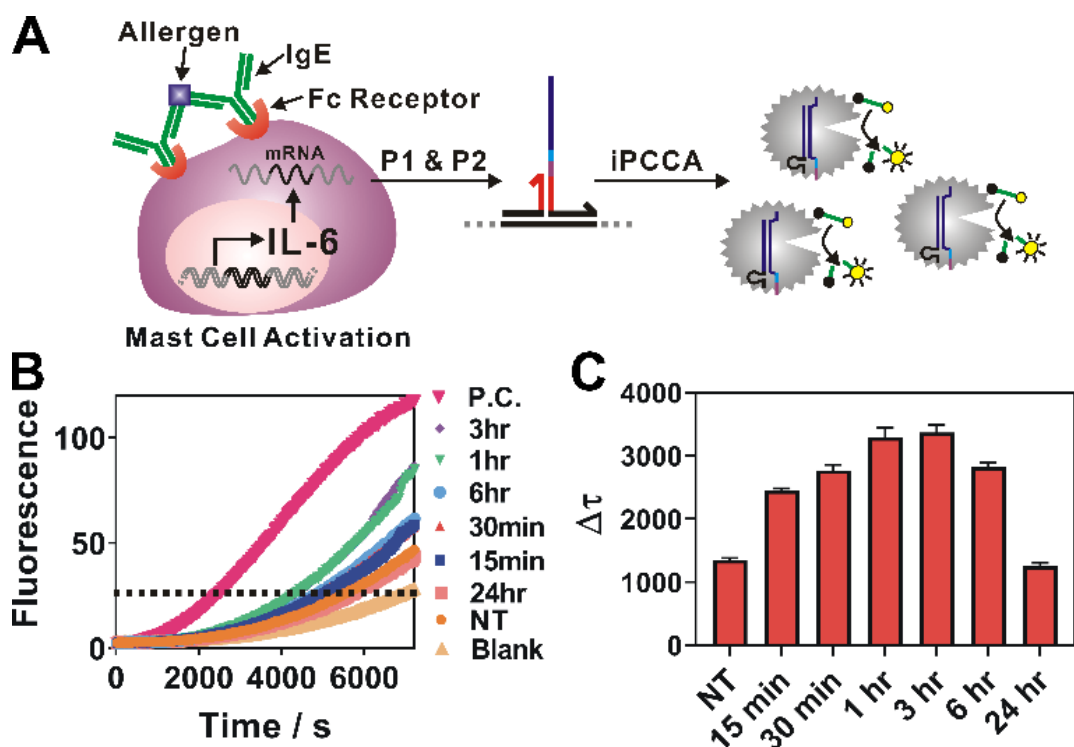


Figure 3.2 (A) Schematic illustration of quantitative profiling of IL-6 expression during allergen-mediated mast cell activation using proximity CRISPR Cas12a assay. (B) Real-time monitoring of the detection of IL-6 mRNA at varying stimulation time points. A threshold was set to determine the critical time τ . $\Delta\tau$ was then determined using $\Delta\tau = 7200s - \tau$. (C) $\Delta\tau$ was normalized against total RNA for samples collected at each stimulation time point and then plotted to determine the temporal changes of IL-6 gene expression during allergen-mediated mast cell activation. Each error bar represents one standard deviation from triplicate analyses (Reprinted with permission from ref ⁶⁶).

As shown in Figure 3.2A, the allergen-mediated mast cell activation was achieved by sensitizing bone marrow-derived mast cells (BMMCs) from wild-type C57BL/6 mice with trinitrophenyl (TNP)-specific IgE and then stimulating the cells using TNP-BSA (allergen) and stem cell factor (SCF) (100 ng/mL) for varying time points (0 min, 15 min, 30 min, 1 hr, 3 hr, 6 hr, and 24 hr). Total RNA was then isolated and quantified directly using proximity CRISPR Cas12a assay. We observed repeatedly that the expression level of IL-6 gene increased upon mast cell activation, peaking at 1-3 hr (Figure 3.2B and 3.2C, Figure 3.3). These observations are highly consistent with our previous observations using reverse transcription and PCR,^{17,18} suggesting that this proximity assay holds the potential to replace PCR as an isothermal alternative for quantifying genetic markers.

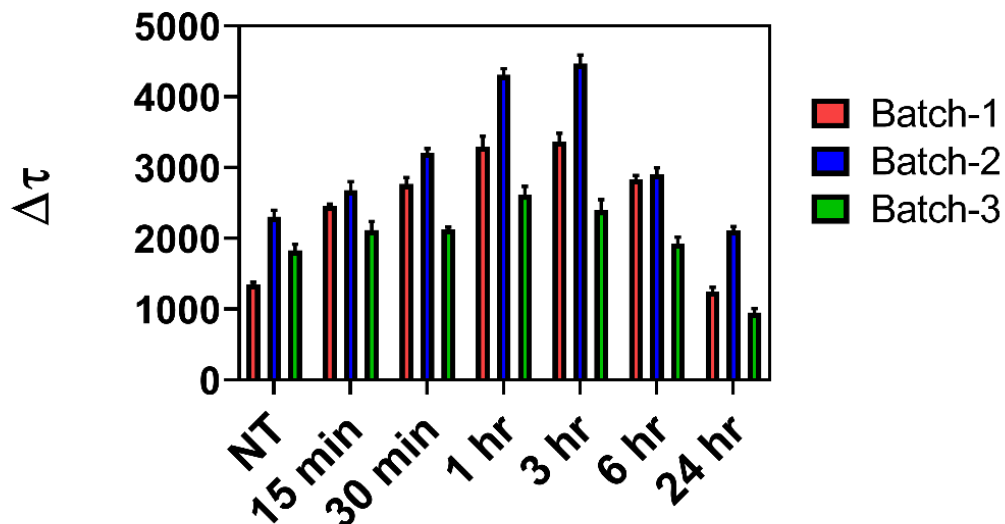


Figure 3.3. Quantitative profiling of allergen-mediated mast cell activation in three independent cultures of BMMCs. The same temporal profiles were obtained from each culture of mast cells sensitized using TNP-specific IgE and stimulated with 100 ng/ml TNP-BSA and SCF for the indicated time points (Reprinted with permission from ref⁶⁶).

3.3.2 Proteins Detections

Having established proximity CRISPR Cas12a assay for the ultrasensitive detection of nucleic acids, we next expand this assay for the amplified detection of proteins. To do so, a pair of affinity ligands that bind to the same target protein but at different epitopes were conjugated to P1 and P2 (noted as P1' and P2'). To allow flexible binding to the target protein, we also designed a 15-nt poly-thymine spacer that separates the ligand and complementary domain (Figure 3.4). Again, the two probes do not hybridize in the absence of the target ($T_m = 17\text{ }^\circ\text{C}$). However, the affinity binding to the target protein brings P1' and P2' into proximity, leading to the formation of a stable duplex (Figure 3.4). As a result, the same CRISPR-targetable DNA barcode can be generated upon proximity primer extension, which activates Cas12a for digesting the fluorogenic substrates.

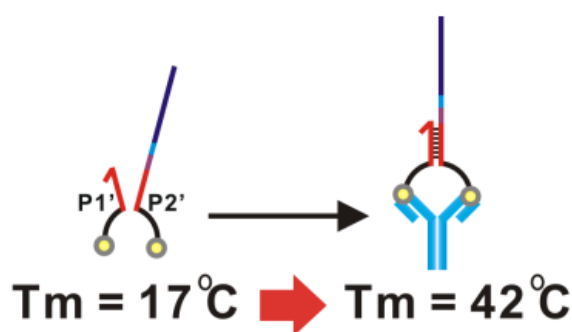


Figure 3.4 Estimated melting temperature (T_m) between P1' and P2' in the absence or presence of the target antibody. In absence of the target antibody, the estimated $T_m = 17\text{ }^\circ\text{C}$ by NuPack, suggesting that P1' and P2' do not hybridize at $37\text{ }^\circ\text{C}$. In the presence of the target, the affinity binding to the target protein brings P1' and P2' into proximity, leading to the formation of a stable duplex with an estimated T_m of $42\text{ }^\circ\text{C}$ (Reprinted with permission from ref ⁶⁶).

As sensitive detection of antibodies in clinical samples plays critical roles for the diagnosis of infectious and autoimmune diseases,⁷²⁻⁷⁴ we chose anti-biotin antibody as a testbed for our assay. Correspondingly, biotin was used as the affinity ligand (Figure 3.5A). In our experiments, concentrations of P1' and P2' and polymerase were found to be critical to maximize the binding-induced primer extension and minimize background (Figure 3.6 and Figure 3.7). We then integrated the assay with nicking endonuclease to further amplify the detection signal. As expected, the concentration of nicking endonuclease also significantly influences the analytical performance of the assay (Figure 3.8). Under optimal experimental conditions, we were able to quantify antibodies with a LOD of 1 pM (Figure 3.5B and Figure 3.5C). Our assay is comparable with commonly used immunoassays in terms of sensitivity but is performed in a homogeneous solution without the need for any immobilization or washing steps. We were also able to quantify antibodies in 10-time diluted human serum samples with a LOD of 10 pM (Figure 3.5D and Figure 3.5E), suggesting that our assay can potentially be adapted to clinical uses.

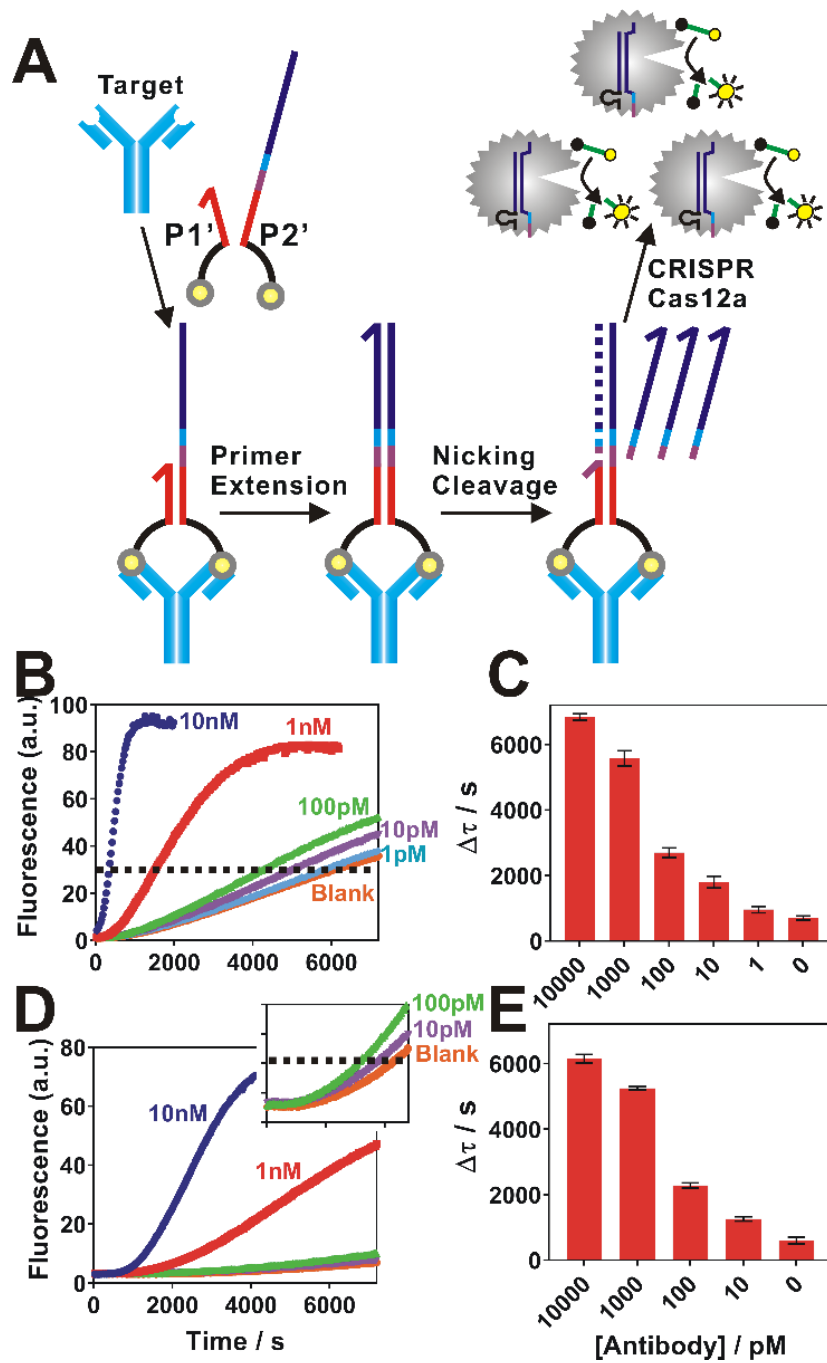


Figure 3.5 Proximity CRISPR Cas12a assay for the detection of antibodies. (A) Schematic illustration of the detection of antibodies using proximity CRISPR Cas12a integrated with nicking cleavage. (B, C) Detection of anti-biotin antibodies with concentrations ranging from 1 pM to 10 nM in buffer. (D, E) Detection of anti-biotin antibodies in 10-time diluted human serum samples. Each error bar represents one standard deviation from triplicate analyses (Reprinted with permission from ref⁶⁶).

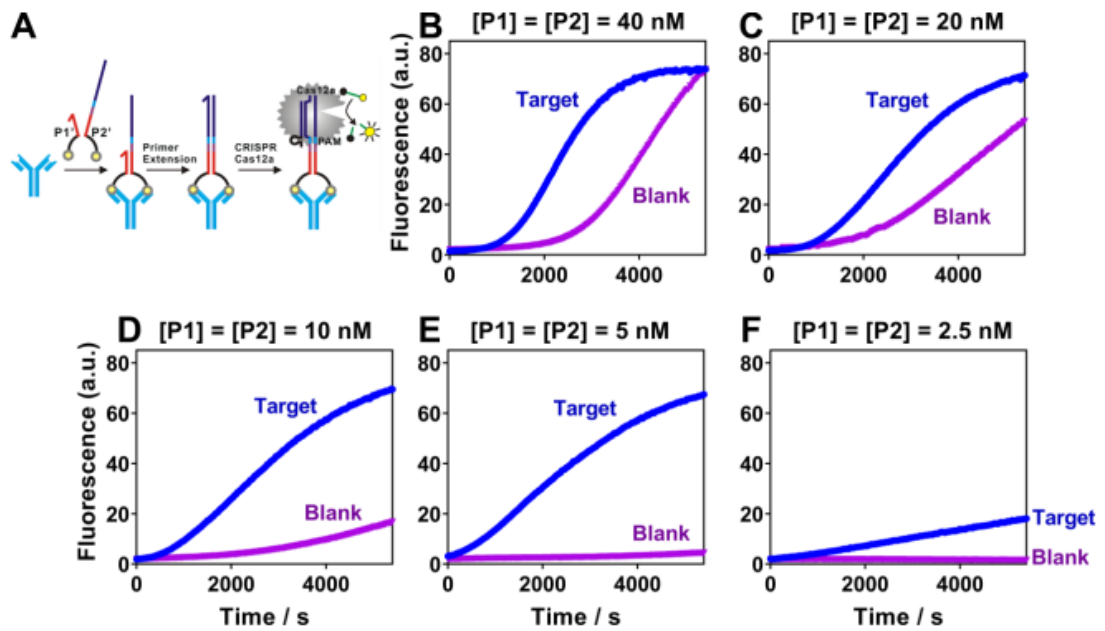


Figure 3.6 Optimization of the concentrations of proximity probes P1' and P2' for protein analysis. (A) Schematic illustration of the detection of protein using a binding-induced primer extension and then CRISPR Cas12a amplification. (B-F) Binding-induced primer extension using varying concentrations of P1' and P2' from 40 nM to 2.5 nM. The optimal concentration of P1' and P2' is 5 nM as it maximizes the target-dependent fluorescence signal and minimizes background signal. [Anti-biotin] = 5 nM, [Polymerase] = 1 U (Reprinted with permission from ref⁶⁶).

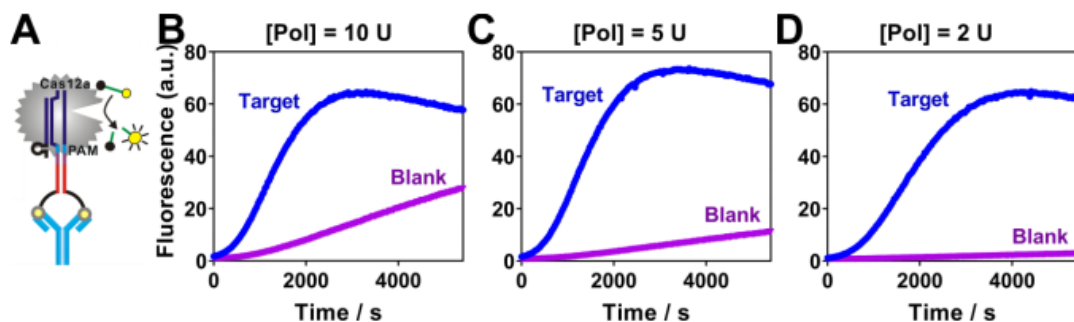


Figure 3.7 Optimization of the concentrations of DNA polymerase (Klenow Fragment, unit) for protein analysis. (A) The detection of protein was achieved using a binding-induced primer extension and then CRISPR Cas12a amplification. (B-D) Detection of anti-biotin antibody using varying concentrations of DNA polymerase. The optimal amount of Klenow Fragment was found to be 5 units, as it maximizes detection signals and kinetics while maintains a reasonably low background. [Anti-biotin] = 5 nM, [P1'] = [P2'] = 5 nM (Reprinted with permission from ref⁶⁶).

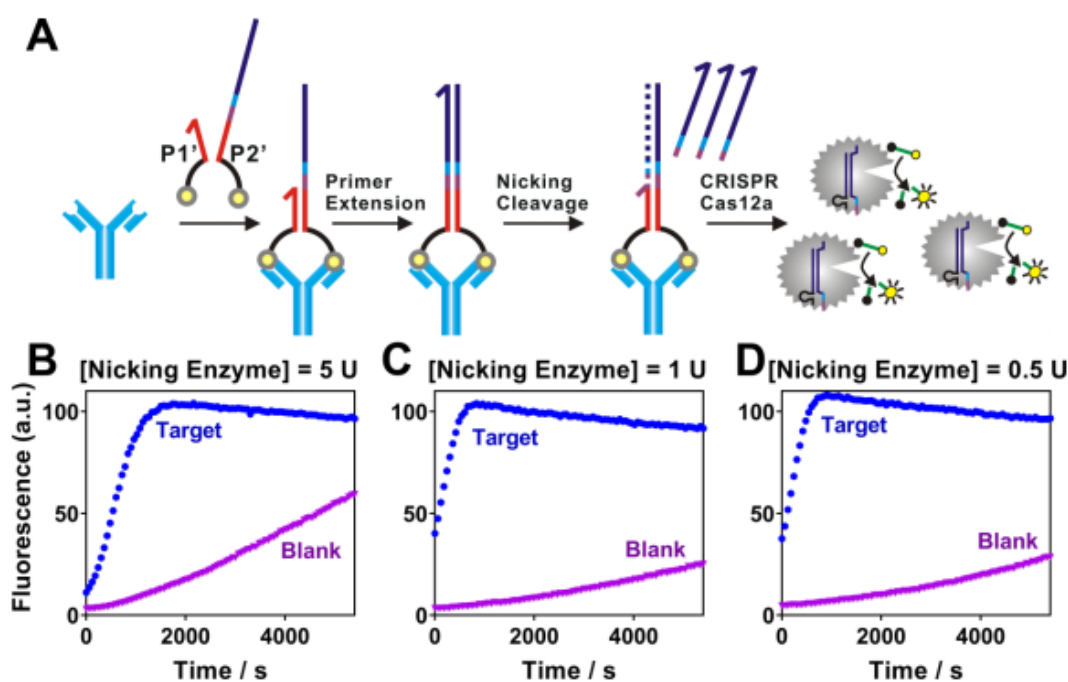


Figure 3.8 Optimization of nicking endonuclease for the proximity CRISPR Cas12a assay. (A) Schematic illustration of antibody detection using proximity CRISPR Cas12a combined with nicking cleavage. (B-D) Detection of anti-biotin antibody using varying concentrations of nicking endonuclease from 0.5 U to 5 U. The optimal amount of nicking endonuclease was found to be 0.5 units, as it maximizes detection signals and minimizes the background. [Anti-biotin] = 5 nM, [P1'] = [P2'] = 5 nM, [Polymerase] = 5 U (Reprinted with permission from ref ⁶⁶).

3.4 Conclusions

In conclusion, we have introduced a proximity CRISPR Cas12a strategy that enables Cas12a as a universal amplifier for the flexible detection of nucleic acids and proteins. DNA has long been recognized as amplifiable barcodes for the ultrasensitive detection of nucleic acids and proteins,⁷⁶⁻⁸⁴ with successful examples ranging from immuno-polymerase chain reactions (PCR),⁷⁶ to proximity ligation/extension assays,⁷⁷⁻⁸⁰ and biobarcode assays.⁸¹⁻⁸⁴ Our proximity CRISPR assay further enriches the toolbox for ultrasensitive biomolecular detection by offering an isothermal, wash-free, and highly

adaptable alternative to the existing ones. Our success in combining CRISPR detection with proximity binding also, for the first time, expands the powerful CRISPR diagnostics (CRISPR Dx) to the sensitive detection of protein-based biomarkers. Our ongoing efforts include to further improve the assay sensitivity by introducing exponential amplification components and to deploy our technology to real clinical and biological samples.

Chapter 4: Conclusion and Future Work

In conclusion, we have successfully developed two CRISPR/Cas12a based biosensing assays for the flexible detection of nucleic acids and proteins. These two CRISPR/Cas12a based biosensing approaches enriched the current toolbox of CRISPR diagnostics (CRISPR Dx) by offering new mechanisms for sequence recognition, signal amplification and result readout. The developed plasmonic CRISPR/Cas12a assay can readily convert standard nucleic acid tests making use of polymerase chain reaction (PCR) or loop-mediated isothermal amplification (LAMP) into a visual, colorimetric test. The developed proximity CRISPR Cas12a assay harnesses collateral ssDNase activity of Cas12a as a universal amplifier for the ultrasensitive detection of nucleic acids and proteins. The target recognition is achieved through proximity binding rather than recognition by crRNA, which allows the flexible assay design and expansion to proteins.

My main research interest lies in the development of rapid, sensitive, portable and cost-efficient CRISPR/Cas based biosensing approaches that can be used in disease diagnosis and field-based applications. Based on my previous projects, my next steps to achieve this goal would be to further improve the performance and robustness of CRISPR/Cas based biosensing approaches by introducing various strategies, such as selecting Cas protein candidates with less sequence restriction (eg. Cas14), integrating with other sensitive isothermal amplification strategies (eg. RPA, RCA) and utilizing more cost-effective colorimetric reagents for result readout (eg. TMB, ABTS).

References

1. Scheler, O., Glynn, B., Kurg, A. Nucleic acid detection technologies and marker molecules in bacterial diagnostics. *Expert Rev. Mol. Diagn.*, **2014**, 14, 489–500.
2. Zhao, Y.X., Chen, F., Li, Q., Wang, L.H., Fan, C.H. Isothermal amplification of nucleic acids. *Chem. Rev.*, **2015**, 115, 12491–12545.
3. Cong, L., Ran, F.A., Cox, D., Lin, S., Barretto, R., Habib, N., Hsu, P.D., Wu, X., Jiang, W., Marraffini, L.A., Zhang, F. Multiplex genome engineering using CRISPR/Cas systems. *Science*, **2013**, 339, 819–823.
4. Mali, P., Yang, L., Esvelt, K.M., Aach, J., Guell, M., DiCarlo, J.E., Norville, J.E., Church, G.M. RNA-guided human genome engineering via Cas9. *Science*, **2013**, 339, 823–826.
5. Zaidi, S.S., Mukhtar M.S., Mansoor, S. Genome editing: targeting susceptibility genes for plant disease resistance. *Trends Biotechnol.*, **2018**, 36(9), 898–906.
6. Ikeda, A., Fujii, W., Sugiura, K. & Naito, K. High-fidelity endonuclease variant HypaCas9 facilitates accurate allele-specific gene modification in mouse zygotes. *Commun. Biol.*, **2019**, 2, 1–7.
7. Lee, C. M., Cradick, T. J. & Bao, G. The *Neisseria meningitidis* CRISPR-Cas9 System Enables Specific Genome Editing in Mammalian Cells. *Mol. Ther.*, **2016**, 24, 645–654.
8. Wright, A.V., Nuñez J.K., Doudna, J.A. Biology and applications of CRISPR systems: harnessing nature’s toolbox for genome engineering. *Cell*, **2016**, 164, 29–44.
9. Sakuma, T., Yamamoto, T. Magic wands of CRISPR lots of choices for gene knock-in. *Cell Biol. Toxicol.*, **2017**, 33, 501–505.
10. Wang, H., La Russa, M., Qi, L.S. CRISPR/Cas9 in genome editing and beyond. *Annu. Rev. Biochem.*, **2016**, 85, 227–264.
11. Pardee, K., Green, A. A., Takahashi, M. K., Braff, D., Lambert, G., Lee, J. W., Ferrante, T., Ma, D., Donghia, N., Fan, M., Daringer, N. M., Bosch, I., Dudley, D. M., O’Connor, D. H., Gehrke, L., Collins, J. J. Rapid, low-cost detection of Zika virus using programmable biomolecular components. *Cell*, **2016**, 165(5), 1255–1266.
12. Makarova, K.S., Haft, D.H., Barrangou, R., Brouns, S.J., Charpentier, E., Horvath, P., Moineau, S., Mojica, F.J., Wolf, Y.I., Yakunin, A.F., van der Oost, J., Koonin, E.V. Evolution and classification of the CRISPR-Cas systems. *Nat. Rev. Microbiol.*, **2011**, 9, 467–477.

13. Jinek, M., Chylinski, K., Fonfara, I., Hauer, M., Doudna, J.A., Charpentier, E. A programmable dual-RNA-guided DNA endonuclease in adaptive bacterial immunity. *Science*, **2012**, 337, 816–821.
14. Koonin, E.V., Makarova, K.S., Zhang, F. Diversity, classification and evolution of CRISPR-Cas systems. *Curr Opin Microbiol.*, **2017**, 37, 67-78.
15. Li, Y., Li, S.Y., Wang, J., Liu, G.Z. CRISPR/Cas Systems towards Next-Generation Biosensing. *Trends in Biotechnology*, **2019**, 37, 7, 730-743.
16. Antonia, A.D., Wendell, A.L., Lei, S.Q. Beyond editing: repurposing CRISPR–Cas9 for precision genome regulation and interrogation. *Nat Rev Mol Cell Biol.*, **2016**, 17(1), 5-15.
17. Brezgin, S., Kostyusheva, A., Kostyushev, D. & Chulanov, V. Dead Cas Systems: Types, Principles, and Applications. *Int. J. Mol. Sci.*, **2019**, 20, 6041.
18. Jiang, W., Bikard, D., Cox, D., Zhang, F. & Marraffini, L. A. RNA-guided editing of bacterial genomes using CRISPR-Cas systems. *Nat. Biotechnol.*, **2013**, 31, 233–239.
19. Zetsche, B., Zetsche, B., Gootenberg, J.S., Abudayyeh, O.O., Slaymaker, I.M., Makarova, K.S., Essletzbichler, P., Volz, S.E., Joung, J., van der Oost, J., Regev, A., Koonin, E.V., Zhang, F. Cpf1 is a single RNA-guided endonuclease of a class 2 CRISPR-Cas system. *Cell*, **2015**, 163, 759–771.
20. Abudayyeh, O.O., Gootenberg, J.S., Essletzbichler, P., Han, S., Joung, J., Belanto, J. J., Verdine, V., Cox, D.B.T., Kellner, M.J., Regev, A., Lander, E.S., Voytas, D.F., Ting, A.Y., Zhang, F. RNA targeting with CRISPRCas13. *Nature*, **2017**, 550, 280–284.
21. Harrington, L.B., Burstein, D., Chen, J.S., Paez-Espino, D., Ma, E., Witte, I.P., Cofsky, J.C., Kyrpides, N.C., Banfield, J.F., Doudna, J.A. Programmed DNA destruction by miniature CRISPR-Cas14 enzymes. *Science*, **2018**, 362, 839–842.
22. Abudayyeh, O.O., Gootenberg, J.S., Konermann, S., Joung, J., Slaymaker, I.M., Cox, D.B., Shmakov, S., Makarova, K.S., Semenova, E., Minakhin, L., Severinov, K., Regev, A., Lander, E.S., Koonin, E.V., Zhang, F. C2c2 is a single-component programmable RNA-guided RNA-targeting CRISPR effector. *Science*, **2016**, 353, aaf5573.
23. Li, S.Y., Cheng, Q.X., Liu, J.K., Nie, X.Q., Zhao, G.P., Wang, J. CRISPR-Cas12a has both cis- and trans-cleavage activities on single-stranded DNA. *Cell Res.*, **2018**, 28, 491–493.
24. Kim, D., Kim, J., Hur, J.K., Been, K.W., Yoon, S., & Kim, J. Genome-wide analysis reveals specificities of Cpf1 endonucleases in human cells. *Nat. Biotechnol.*, **2016**,

- 34, 863–868.
25. Compton, J. Nucleic acid sequence-based amplification. *Nature*, **1991**, 350(6313), 91-92.
 26. Green, A.A., Silver, P.A., Collins, J.J., Yin, P. Toehold switches: de-novo-designed regulators of gene expression. *Cell*, **2014**, 159, 925–939.
 27. Wang, Q., Zhang, B., Xu, X., Long, F., Wang, J. CRISPR-typing PCR (ctPCR), a new Cas9-based DNA detection method. *Sci. Rep.*, **2018**, 8, 14126.
 28. Quan, J., Langelier, C., Kuchta, A., Batson, J., Teyssier, N., Lyden, A., Caldera, S., McGeever, A., Dimitrov, B., King, R., Wilhelm, J., Murphy, M., Ares, L.P., Travisano, K.A., Sit, R., Amato, R., Mumbengegwi, D.R., Smith, J.L., Bennett, A., Gosling, R., Mourani, P.M., Calfee, C.S., Neff, N.F., Chow, E.D., Kim, P.S., Greenhouse, B., DeRisi, J.L., Crawford, E.D. FLASH: a next-generation CRISPR diagnostic for multiplexed detection of antimicrobial resistance sequences. *Nucleic Acids Res.*, **2019**, 47(14), e83.
 29. Zhang, Y. & Zhang, C. Sensitive detection of microRNA with isothermal amplification and a singlequantum-dot-based nanosensor. *Anal. Chem.*, **2012**, 84, 224–231.
 30. Huang, M. Q., Zhou, X. M., Wang, H. Y., Xing, D. Clustered regularly interspaced short palindromic repeats/Cas9 triggered isothermal amplification for site-specific nucleic acid detection. *Analytical Chemistry*, **2018**, 90, 2193–2200.
 31. Zhou, W., Hu, L., Ying, L., Zhao, Z., Chu, P. K., Yu, X. F. A CRISPR–Cas9-triggered strand displacement amplification method for ultrasensitive DNA detection. *Nature Communications*, **2018**, 9(1), 1–11.
 32. Zhang, Y., Qian, L., Wei, W.J., Wang, Y., Wang, B.N., Lin, P.P., Liu, W.C., Xu, L.Z., Li, X., Liu, D.M., Cheng, S.D., Li, J.F., Ye, Y.X., Li, H., Zhang, X.H., Dong, Y.M., Zhao, X.J., Liu, C.H., Zhang, H.Q.M., Ouyang, Q., Lou, C.B. Paired design of dCas9 as a systematic platform for the detection of featured nucleic acid sequences in pathogenic strains. *ACS Synthetic Biology*, **2017**, 6, 211–216.
 33. Qiu, X.Y., Zhu, L.Y., Zhu, C.S., Ma, J.X., Hou, T., Wu, X.M., Xie, S.S, Min, L., Tan, D.A., Zhang, D.Y., Zhu, L.Y. Highly effective and low-cost microRNA detection with CRISPR-Cas9. *ACS Synthetic Biology*, **2018**, 7, 807–813.
 34. Hajian, R., Balderston, S., Tran, T., deBoer, T., Etienne, J., Sandhu, M., Wauford, N.A., Chung, J.Y., Nokes, J., Athaiya, M., Paredes, J., Peytavi, R., Goldsmith, B., Murthy, N., Conboy, I.M., Aran, K. Detection of unamplified target genes via CRISPR–Cas9 immobilized on a graphene field-effect transistor. *Nature Biomedical Engineering*, **2019**, 3, 427–437.

35. Chen, J.S., Ma, E.B., Harrington, L.B., Costa, M.D., Tian, X.R., Palefsky, J.M., Doudna, J.A. CRISPR-Cas12a target binding unleashes indiscriminate single-stranded DNase activity. *Science*, **2018**, 360, 436–439.
36. Li, S.Y., Cheng, Q.X., Wang, J.M., Li, X.Y., Zhang, Z.L., Gao, S., Cao, R.B., Zhao, G.P., Wang, J. CRISPR-Cas12a-assisted nucleic acid detection. *Cell Discovery*, **2018**, 4, 20.
37. Li, L.X., Li, S.Y., Wang, J. CRISPR-Cas12b-assisted nucleic acid detection platform. *bioRxiv*, **2018**, 362889.
38. Li, L., Li, S., Wu, N., Wu, J., Wang, G., Zhao, G., Wang, J. HOLMESv2: A CRISPR-Cas12b-Assisted Platform for Nucleic Acid Detection and DNA Methylation Quantitation. *ACS Synth. Biol.*, **2019**, 8(10), 2228–2237.
39. Dai, Y., Somoza, R.A., Wang, L., Welter, J.F., Li, Y., Caplan, A.I., Liu, C.C. Exploring the Trans-Cleavage Activity of CRISPR-Cas12a (cpf1) for the Development of a Universal Electrochemical Biosensor. *Angew. Chemie Int. Ed.*, **2019**, 58, 17399–17405.
40. East-Seletsky, A., O'Connell, M.R., Knight, S.C., Burstein, D., Cate, J.H., Tjian, R., Doudna, J.A. Two distinct RNase activities of CRISPR-C2c2 enable guide-RNA processing and RNA detection. *Nature*, **2016**, 538, 270–273.
41. Gootenberg, J.S., Abudayyeh, O.O., Lee, J.W., Essletzbichler, P., Dy, A.J., Joung, J., Verdine, V., Donghia, N., Daringer, N.M., Freije, C.A., Myhrvold, C., Bhattacharyya, R.P., Livny, J., Regev, A., Koonin, E.V., Hung, D.T., Sabeti, P.C., Collins, J.J., Zhang, F. Nucleic acid detection with CRISPR-Cas13a/C2c2. *Science*, **2017**, 356, 438–442.
42. Gootenberg, J.S., Abudayyeh, O.O., Kellner, M.J., Joung, J., Collins, J.J., Zhang, F. Multiplexed and portable nucleic acid detection platform with Cas13, Cas12a, and Csm6. *Science*, **2018**, 360(6387), 439–444.
43. Myhrvold, C., Freije, C.A., Gootenberg, J.S., Abudayyeh, O.O., Metsky, H.C., Durbin, A.F., Kellner, M.J., Tan, A.L., Paul, L.M., Parham, L.A., Garcia, K.F., Barnes, K.G., Chak, B., Mondini, A., Nogueira, M.L., Isern, S., Michael, S.F., Lorenzana, I., Yozwiak, N.L., MacInnis, B.L., Bosch, I., Gehrke, L., Zhang, F., Sabeti, P.C. Field-deployable viral diagnostics using CRISPR-Cas13. *Science*, **2018**, 360, 444–448.
44. Li, Y.; Mansour, H.; Wang, T.; Poojari, S.; Li, F. Naked-eye detection of grapevine red-blotch viral infection using a plasmonic CRISPR Cas12a assay. *Analytical Chemistry*, **2019**, 91, 18, 11510–11513.
45. Lipsitch, M.; Cohen, T.; Cooper, B.; Robins, J. M.; Ma, S.; James, L.;

- Gopalakrishna, G.; Chew, S. K.; Tan, C. C.; Samore, M. H.; Fisman, D.; Murray, M. Transmission dynamics and control of severe acute respiratory syndrome. *Science* **2003**, 300, 1966-1970.
46. Petersen, L. R.; Jamieson, D. J.; Powers, A. M.; Honein, M. A. Zika virus. *N. Engl. J. Med.* **2016**, 374, 1552-1564.
47. Sullivan, S. J.; Jacobson, R. M.; Dowdle, W. R.; Poland, G. A. 2009 H1N1 influenza. *Mayo Clin. Proc.* **2010**, 85, 64–76.
48. Liang, T. J. Hepatitis B: The Virus and Disease. *Hepatology* **2009**, 49, 13–21.
49. Cieniewicz, E. J.; Pethybridge, S. J.; Loeb, G.; Perry, K.; Fuchs, M. Insights into the ecology of grapevine red blotch virus in a diseased vineyard. *Phytopathology*. **2018**, 108, 94–102.
50. Niemz, A.; Ferguson, T. M.; Boyle, D. S. Point-of-care nucleic acid testing for infectious diseases. *Trends in Biotechnol.* **2011**, 29, 240–250.
51. Dong, T.; Wang, G. A.; Li, F. Shaping up field-deployable nucleic acid testing using microfluidic paper-based analytical devices. *Anal. Bioanal. Chem.* **2019**, DOI: 10.1007/s00216-019-01595-7
52. Lin, M.; Pei, H.; Yang, F.; Fan, C.; Zuo, X. Applications of gold nanoparticles in the detection and identification of infectious diseases and biothreats. *Adv. Mat.* **2013**, 25, 3490–3496.
53. Elghanian, R.; Storhoff, J. J.; Mucic, R. C.; Letsinger, R. L.; Mirkin, C. A. Selective colorimetric detection of polynucleotides based on the distance-dependent optical properties of gold nanoparticles. *Science* **1997**, 277, 1078–1081.
54. Zagorovsky, K.; Chan, W. C. W. A plasmonic DNAzyme strategy for point-of-care genetic detection of infectious pathogens. *Angew. Chem. Int. Ed.* **2013**, 52, 3168.
55. Valentini, P., Pompa, P. P. A universal polymerase chain reaction developer. *Angew. Chem. Int. Ed.* **2016**, 55, 2157-2161.
56. Deng, H.; Xu, Y.; Liu, Y.; Guo, H.; Shan, S.; Sun, Y.; Liu, X.; Huang, K.; Ma, X.; Wu, Y.; Liang, X. J. Gold nanoparticles with asymmetric polymerase chain reaction for Colorimetric Detection of DNA Sequence. *Anal. Chem.* **2012**, 84, 1253-1258.
57. Seferos, D. S.; Giljohann, D. A.; Hill, H. D.; Prigodich, A. E.; Mirkin, C. A. Nanoflares: probes for transfection and mRNA detection in living cells. *J. Am. Chem. Soc.* **2007**, 129, 15477-15480.
58. Prigodich, A. E.; Randeria, P. S.; Briley, W. E.; Kim, N. J.; Daniel, W. L.; Giljohann, D. A.; Mirkin, C. A. Multiplexed nanoflares: mRNA detection in live cells. *Anal. Chem.* **2012**, 84, 2062-2066.

59. Song, T.; Xiao, S.; Yao, D.; Huang, F.; Hu, M.; Liang, H. An efficient DNA-fueled molecular machine for the discrimination of single-base changes. *Adv. Mat.* **2014**, *26*, 6181-6185.
60. Mao, X.; Ma, Y.; Zhang, A.; Zhang, L.; Zeng, L.; Liu, G. Disposable Nucleic Acid Biosensors Based on Gold Nanoparticle Probes and Lateral Flow Strip. *Anal. Chem.* **2009**, *81*, 1660–1668.
61. Zetsche, B.; Gootenberg, J. S.; Abudayyeh, O. O.; Slaymaker, I. M.; Makarova, K. S.; Essletzbichler, P.; Volz, S. E.; Joung, J.; van der Oost, J.; Regev, A.; Koonin, E.; Zhang, F. Cpf1 Is a Single RNA-guided Endonuclease of a Class 2 CRISPR-Cas System. *Cell* **2015**, *163*, 759–771.
62. Chen, J. S.; Ma, E.; Harrington, L. B.; Da Costa, M.; Tian, X.; Palefsky, J. M.; Doudna, J. A. CRISPR-Cas12a target binding unleashes indiscriminate single-stranded DNase activity. *Science* **2018**, *360*, 436-440.
63. Krenz, B.; Thompson, J. R.; Fuchs, M.; Perry, K. L. Grapevine red blotch-associated virus Is Widespread in the United States. *Phytopathology* **2014**, *104*, 1232-1240.
64. Wang, H.; Kim, S.; Ryu, W.S. DDX3 DEAD-Box RNA helicase inhibits Hepatitis B Virus reverse transcription by incorporation into nucleocapsids. *Journal of Virology* **2009**, *83*, 5815-5824.
65. Nyan, D. C.; Ulitzky, L. E.; Cehan, N.; Williamson, P.; Winkelman, V.; Rios, M.; Taylor, D. R. Rapid detection of Hepatitis B Virus in blood plasma by a specific and sensitive loop-mediated isothermal amplification assay *Clin. Infect. Dis.* **2014**, *59*, 16–23.
66. Li, Y.; Mansour, H.; Tang, Y.; Li, F. A universal proximity CRISPR Cas12a assay for ultrasensitive detection of nucleic acids and proteins. *BioRxiv*, **2019**, 734582, doi: <https://doi.org/10.1101/734582>.
67. Zuo, X.; Fan, C.; Chen, H.-Y. Biosensing: CRISPR-powered diagnostics. *Nat. Biomed. Eng.*, **2017**, *1*, 0091.
68. Shmakov, S.; Smargon, A.; Scott, D.; Cox, D.; Pyzocha, N.; Yan, W.; Abudayyeh, O. O.; Gootenberg, J. S.; Makarova, K. S.; Wolf, Y. I.; Severinov, K.; Zhang, F.; Koonin, E. V. Diversity and evolution of class 2 CRISPR-Cas systems. *Nat. Rev. Microbiol.*, **2017**, *15*, 169-182.
69. Gootenberg, J. S.; Abudayyeh, O. O.; Lee, J. W.; Essletzbichler, P.; Dy, A. J.; Joung, J.; Verdine, Y.; Donghia, N.; Daringer, N. M.; Freije, C. A.; Myhrvold, C.; Bhattacharyya, R. P.; Livney, J.; Regev, A.; Koonin, E. V.; Hung, D. T.; Sabeti, P. C.; Collins, J. J.; Zhang, F. Nucleic acid detection with CRISPR-Cas13a/C2c2.

- Science*, **2017**, 365, 438-442.
70. Gootenberg, J. S.; Abudayyeh, O. O.; Kellner, M. J.; Joung, J.; Collins, J. J.; Zhang, F. Multiplexed and portable nucleic acid detection platform with Cas13, Cas12a, and Csm6. *Science*, **2018**, 360, 439-444.
 71. Myhrvold, C.; Freije, C. A.; Gootenberg, J. S.; Abudayyeh, O. O.; Metsky, H. C.; Durbin, A. F.; Kellner, M. J.; Tan, A. L.; Paul, L. M.; Parham, L. A.; Garcia, K. F.; Barnes, K. G.; CHak, B.; Mondini, A.; Nogueira, M. L.; Isern, S.; Michael, S. F.; Lorenzana, I.; Yozwiak, N. L.; MacInnis, B. L.; Bosch, I.; Gehrke, L.; Zhang, F.; Sabeti, P. C. Field-deployable viral diagnostics using CRISPR-Cas13. *Science*, **2018**, 360, 444-448.
 72. Chen, J. S.; Ma, E.; Harrington, L. B.; Costa, M. D.; Tian, X.; Palefsky, J. M.; Doudna, J. A. CRISPR-Cas12a target binding unleashes indiscriminate single-stranded DNase activity. *Science*, **2018**, 360, 436-439.
 73. Meroni, P. L.; Biggioggero, M.; Pierangeli, S. S.; Sheldon, J.; Zegers, I.; Borghi, M. O. Standardization of autoantibody testing: a paradigm for serology in rheumatic diseases. *Nat. Rev. Rheumatol.*, **2014**, 10, 35-43.
 74. Porchetta, A.; Ippodrino, R.; Marini, B.; Caruso, A.; Caccuri, F.; Ricci, F. Programmable nucleic acid nanoswitches for the rapid, single-step detection of antibodies in bodily fluids. *J. Am. Chem. Soc.*, **2018**, 140, 947-953.
 75. Tsai, C.; Robinson, P. V.; Spencer, C. A.; Bertozzi, C. R. Ultrasensitive antibody detection by agglutination-PCR (ADAP). *ACS Cent. Sci.*, **2016**, 2, 139-147.
 76. Zhang, H.; Li, F.; Dever, B.; Li, X.-F.; Le, X. C. DNA-mediated homogeneous binding assays for nucleic acids and proteins. *Chem. Rev.*, **2013**, 113, 2812-2841.
 77. Sano, T.; Smith, C. L.; Cantor, C. R. Immuno-PCR: very sensitive antigen detection by means of specific antibody-DNA conjugates. *Science*, **1992**, 258, 120-122.
 78. Fredriksson, S.; Gullberg, M.; Jarvius, J.; Olsson, C.; Pietras, K.; Gustafsdottir, S. M.; Ostman, A.; Landegren, U. Protein detection using proximity-dependent DNA ligation assays. *Nat. Biotechnol.*, **2002**, 20, 473-477.
 79. Soderberg, O.; Gullberg, M.; Jarvius, M.; Ridderstrale, K.; Leuchowius, K.-J.; Jarvius, J.; Wester, K.; Hydbring, P.; Bahram, F.; Larsson, L.-G.; Landegren, U. Direct observation of individual endogenous protein complexes in situ by proximity ligation. *Nat. Methods*, **2006**, 12, 995-1000.
 80. Lundberg, M.; Eriksson, A.; Tran, B.; Assarsson, E.; Fredriksson, S. Homogeneous antibody-based proximity extension assays provide sensitive and specific detection of low-abundant proteins in human blood. *Nucleic Acid Res.*, **2011**, 39, e102.

81. Zhang, H.; Li, F.; Dever, B.; Wang, C.; Li, X.-F.; Le, X. C. Assembling DNA through affinity binding to achieve ultrasensitive protein detection. *Angew. Chem. Int. Ed.*, **2013**, 52, 10698-10705.
82. Nam, J. M.; Thaxton, C. S.; Mirkin, C. A. Nanoparticle-based bio-bar codes for the ultrasensitive detection of proteins. *Science*, **2003**, 301, 1884-1886.
83. Thaxton, C. S.; Elghanian, R.; Thomas, A. D.; Stoeva, S. I.; Lee, J.-S.; Smith, N. D.; Schaeffer, A. J.; Klocker, H.; Horninger, W.; Bartsch, G.; Mirkin, C. A. Nanoparticle-based bio-barcode assay redefines "undetectable" PSA and biochemical recurrence after radical prostatectomy. *Proc. Natl. Acad. Sci. U. S. A.*, **2009**, 106, 18437-18442.
84. Li, F.; Lin, Y.; Lau, A.; Tang, Y.; Chen, J. X.; Le, C. Binding-induced molecular amplifier as a universal detection platform for biomolecules and biomolecular interaction. *Anal. Chem.*, **2018**, 90, 8651-8657.